

University of Windsor

Scholarship at UWindor

Electronic Theses and Dissertations

Theses, Dissertations, and Major Papers

1-1-1970

Quarter-wave filters on transmission lines.

Eckhard Denzinger
University of Windsor

Follow this and additional works at: <https://scholar.uwindsor.ca/etd>

Recommended Citation

Denzinger, Eckhard, "Quarter-wave filters on transmission lines." (1970). *Electronic Theses and Dissertations*. 6615.

<https://scholar.uwindsor.ca/etd/6615>

This online database contains the full-text of PhD dissertations and Masters' theses of University of Windsor students from 1954 forward. These documents are made available for personal study and research purposes only, in accordance with the Canadian Copyright Act and the Creative Commons license—CC BY-NC-ND (Attribution, Non-Commercial, No Derivative Works). Under this license, works must always be attributed to the copyright holder (original author), cannot be used for any commercial purposes, and may not be altered. Any other use would require the permission of the copyright holder. Students may inquire about withdrawing their dissertation and/or thesis from this database. For additional inquiries, please contact the repository administrator via email (scholarship@uwindsor.ca) or by telephone at 519-253-3000ext. 3208.

INFORMATION TO USERS

This manuscript has been reproduced from the microfilm master. UMI films the text directly from the original or copy submitted. Thus, some thesis and dissertation copies are in typewriter face, while others may be from any type of computer printer.

The quality of this reproduction is dependent upon the quality of the copy submitted. Broken or indistinct print, colored or poor quality illustrations and photographs, print bleedthrough, substandard margins, and improper alignment can adversely affect reproduction.

In the unlikely event that the author did not send UMI a complete manuscript and there are missing pages, these will be noted. Also, if unauthorized copyright material had to be removed, a note will indicate the deletion.

Oversize materials (e.g., maps, drawings, charts) are reproduced by sectioning the original, beginning at the upper left-hand corner and continuing from left to right in equal sections with small overlaps.

ProQuest Information and Learning
300 North Zeeb Road, Ann Arbor, MI 48106-1346 USA
800-521-0600

UMI[®]

QUARTER-WAVE FILTERS ON TRANSMISSION LINES

by

Eckhard Denzinger

A Thesis

Submitted to the Faculty of Graduate Studies through the
Department of Electrical Engineering in Partial Fulfillment
of the Requirements for the Degree of
Master of Applied Science at the
University of Windsor

Windsor, Ontario
1970

UMI Number:EC52794

UMI[®]

UMI Microform EC52794
Copyright 2007 by ProQuest Information and Learning Company.
All rights reserved. This microform edition is protected against
unauthorized copying under Title 17, United States Code.

ProQuest Information and Learning Company
789 East Eisenhower Parkway
P.O. Box 1346
Ann Arbor, MI 48106-1346

AAX 7869

Approved: A. L. L.

 P. H. Head

 C. Samuel

 W. C. Perry

322765

ABSTRACT

Quarter-wave H.F. filters were originally developed and studied on a single-conductor test line in Japan¹. Subsequently, the filters were installed on a 250-kV, three-phase line. In this thesis a general analysis of quarter-wave filters is described. The analysis is then applied to the study of filter performance on single-, two- and three-phase full-scale lines. These filters are of the narrow-band type but when in cascade and staggered-tuned, they provide good attenuation over a broad band of frequencies.

ACKNOWLEDGEMENT

The author would like to express his sincere gratitude to his supervisor Prof. M. C. Perz for guidance and continued inspiration throughout the course of the research.

The author is indebted to the National Research Council of Canada for financial support of the research in the form of a scholarship.

INTRODUCTION

The most familiar H.F. filters on powers lines are the lumped-parameter tuned filters for power line carrier (PLC) applications. These filters are inserted in series with the phase conductor and, hence, must be designed to withstand the high short-circuit fault currents. Furthermore, these filters are operating at the line potential and require insulated installation that might be quite expensive at EHV.

The quarter-wave (Q-W) filters, originally investigated in Japan¹, consist of hollow light conductors suspended under each phase at a distance of one to two feet. The basic length of the stub is about one span at 200kHz. The stub does not carry the line current. Sawada and Nakamura¹ proposed an equivalent circuit for a Q-W filter on a single-phase line and from this equivalent circuit developed equations for the filter attenuation. The calculated results were confirmed by measurements made on a model line. The findings were so encouraging that subsequently a system of staggered filters has been installed on a 250-kV line. Field intensity measurements under this line indicate that the Q-W filters are practical and provide a means for substantially reducing HF signals over a broad band of frequencies. The performance of these filters were found very satisfactory during a two-year operation.

The equations developed by Sawada and Nakamura are approximate only and applicable to a single-conductor power line. Hence, a general and exact analysis for multiphase lines seemed

to be of practical interest.

The proposed analysis demonstrates solutions of boundary problems on multiconductor systems and, hence, with some modifications may find other useful applications.

Two methods are developed, one, called the Direct Method, that makes use of generalized passive circuit network theory. In particular, input admittance matrices are developed at each line discontinuity. In the other one, called the Detailed Method, the conductor voltage and current components are resolved into incident and reflected quantities. The application of boundary conditions and propagation equations in this method leads to a system of simultaneous equations; their solution provides the information necessary to find the filter attenuation.

Calculated results using the analysis developed here are compared with some experimental results of model test lines in Japan. The analysis is further applied to a single-, two- and three-phase full scale lines to study the influence of various parameters on the filter performance.

The use of matrix equations throughout this work greatly simplifies the expressions involved. However, the actual numerical solution even of the single-phase line requires the use of a computer or advanced desk calculator because the elements of most of the matrices are complex and vary with frequency.

TABLE OF CONTENTS

ABSTRACT.....	iii
ACKNOWLEDGEMENTS.....	iv
INTRODUCTION.....	v
 Chapter	
I. GENERAL CONSIDERATIONS.....	1
II. DIRECT METHOD.....	5
Solution of the Boundary Value Problem.....	6
Evaluation of Attenuation.....	17
III. DETAILED METHOD.....	21
IV. THE SAWADA AND NAKAMURA METHOD. COMPARISON BETWEEN CALCULATED AND EXPERIMENTAL RESULTS...	30
The Sawada and Nakamura Method.....	30
Experimental Results.....	32
V. FILTER PERFORMANCE ON FULL SCALE LINES.....	37
Single Phase Line.....	37
Effect of Termination on Frequency Response.....	37
Effect of Filter Geometry.....	43
Performance on Multiphase Lines.....	46
VI. RESUME AND CONCLUSIONS.....	52
REFERENCES.....	54
APPENDIX A DIRECT METHOD.....	55
APPENDIX B CAPACITIVE TERMINATION.....	58

CHAPTER I
GENERAL CONSIDERATIONS

The lines before and after the filter may be different but still of the same number of main conductors. Figure 1 represents such an arrangement. Line 1, the portion of the power line to the left of T consists of N conductors and so does Line 3, the power line to the right of R. The filter is connected between T and R and can be regarded as a $2N$ conductor line of length L , terminated at both ends.

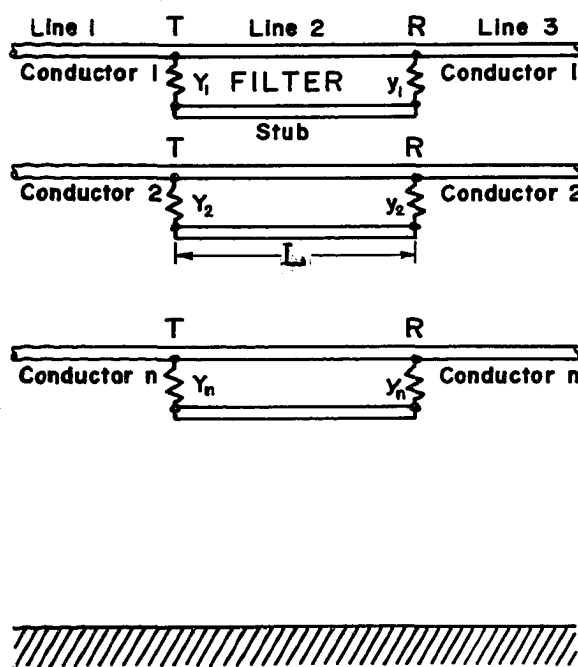


Fig. 1. Q-W Filters on Multiphase Lines

In a more general case there may be two or more stubs per one main conductor and the latter may be a bundle of subconductors, but the analysis would still follow the same lines.

To simplify the analysis, the following assumptions are made:

- (1) Since Line 2 is short, it is considered to be lossless.
- (2) Proximity effect between all conductors of the filter are neglected.
- (3) End effects (field distortion) due to discontinuities at T and R are neglected.

Because of the number of variables involved, the matrix notation will be used.

For example

$$[V] = [Z][I] \quad (1)$$

means

$$\begin{bmatrix} V_1 \\ V_2 \\ \cdot \\ \cdot \\ \cdot \\ V_N \end{bmatrix} = \begin{bmatrix} Z_{11} & Z_{12} & \dots & Z_{1N} \\ \cdot & & & \\ \cdot & & & \\ \cdot & & & \\ \cdot & & & \\ Z_{N1} & \dots & & Z_{NN} \end{bmatrix} \begin{bmatrix} I_1 \\ \cdot \\ \cdot \\ \cdot \\ \cdot \\ I_N \end{bmatrix}$$

where the V_i , $i = 1, \dots, N$ are the conductor to ground voltages and the I_i , $i = 1, \dots, N$ are conductor currents in the positive direction. In most equations and figures the brackets of the matrix notation will be omitted so that equation (1) becomes

$$V = ZI \quad (2)$$

The multiconductor line in Figure 1 can thus be represented by a symbolic single-conductor line as in Figure 2 (Chapter 2), where for clarity, the boundaries T and R have been "stretched".

Capital letters are used for quantities at the boundary T, lower case letters for quantities at the boundary R. On Line 2 the subscript l (l for line) refers to main conductor quantities, the subscript s (s for stub) to stub quantities.

The analysis of the Direct Method consists of two parts. In the first part, matrix equations are derived that relate the voltage v_D and current i_D after the filter, Figure 2, to the voltage V_A and current I_A before the filter.

The voltage at A, V_A , is different in the presence of the filter from the voltage that would exist in absence of the filter. To assess the attenuation properties of the filter, it is necessary to relate the voltage v_D to the voltage V'_A that would exist at A in the absence of the filter when Line 3 is directly connected to Line 1 at A. This is done in the second part of the analysis where the relation between the voltages V_A and V'_A in the presence and in the absence of the filter is determined.

In the Detailed Method a system of simultaneous complex linear matrix equations in terms of current and voltage waves is derived. The + superscript is used for voltage and current waves travelling in the positive direction, to the right in Figure 4 (Chapter 3), the - superscript for waves travelling in the negative direction, to the left. The equations for the voltage and current waves at any point of the line are

$$V = V^+ + V^- \quad (3)$$

$$I = I^+ + I^- \quad (4)$$

where V and I are column matrices. The analysis is derived for the case where Line 1 and Line 3 are identical and reflection-free at their far ends. The system of equations is solved for all wave quantities in terms of the incident voltage V^+ . V^+ is also the line voltage in absence of the filter, because the line is reflection-free. Hence the relation between v^+ and V^+ directly specifies the attenuation properties of the filter.

As outlined in Chapter 3, the analysis can be extended to solve the general case of Lines 1 and 3 being different and not reflection-free.

For the numerical examples given, most calculations were made using the Direct Method which requires the operation of complex matrices of the order $2N$, where N is the number of main conductors. The Detailed Method which requires the operation of complex matrices of at least the order $10N$ was used to check out the results. "Matlan", a matrix oriented computer language for the IBM 360 computer, was used in the calculations.

CHAPTER II
DIRECT METHOD

The analysis is developed in several steps. First, boundary conditions at R, Figure 2, are determined from nodal current matrix equations². These allow the nodal currents i_ℓ and i_s to be expressed in terms of nodal voltages, v_ℓ and v_s , through the effective admittance matrix y . Because of the voltage continuity at C-D, components of v_ℓ are equal to the actual conductor voltages v_D of Line 3 in the presence of the filter.

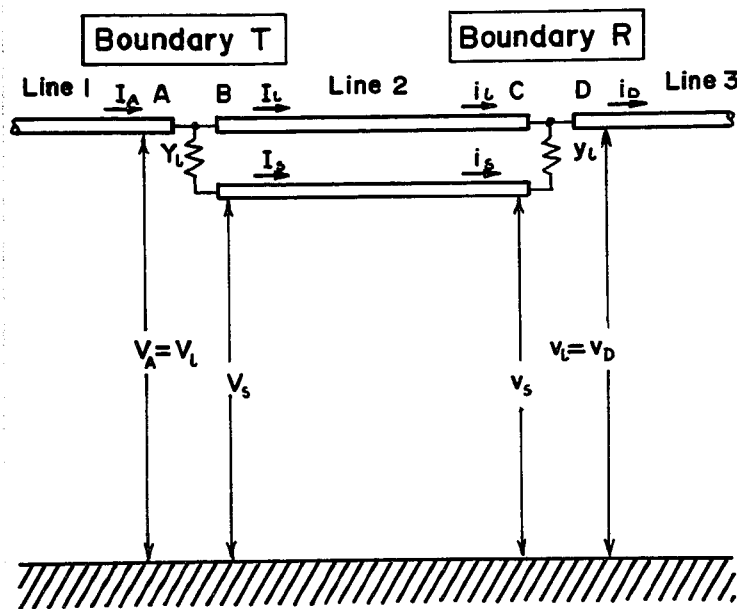


Fig. 2. Diagram of the Reduced System in Figure 1.

Next, equations for voltages and currents at B in terms of voltages and currents at C are derived. These equations make use of the a, b, c, d network constants in matrix form³ applied to Line 2 of length L . From the first two steps various forms of the admittance and impedance matrices, Y_B and z_B , of the filter to the right of B are found.

In the third step, the admittance matrix Y , that includes the terminating admittance Y_L between the main conductors and the stubs at boundary T is developed. Hence, the currents I_A and voltages V_A of Line 1, can be related to the voltages v_D or current i_D of line 3 after the filter.

Finally, the voltages V_A are found in terms of voltages V'_A that would exist at A in the absence of the filter, as though Line 3 was directly connected to Line 1. As a result, the voltages v_D after the filter can be compared with the voltages V'_A at any desired frequency. Thus, the attenuation properties of the filter can be assessed.

Solution of the boundary value problem.

To illustrate the derivation of the effective terminating admittance matrix $[y]$ at boundary R the nodal current network for a two-conductor Line 3 is shown in Figure 3. Let the Y_3 be the input admittance matrix of Line 3 that may be reflection-free or terminated, and Z_3 be the inverse of Y_3 , $Z_3 = Y_3^{-1}$. For the main conductors counted from one to n , and the stubs $(n + 1)$ to $(n + n)$, the column vectors can be partitioned

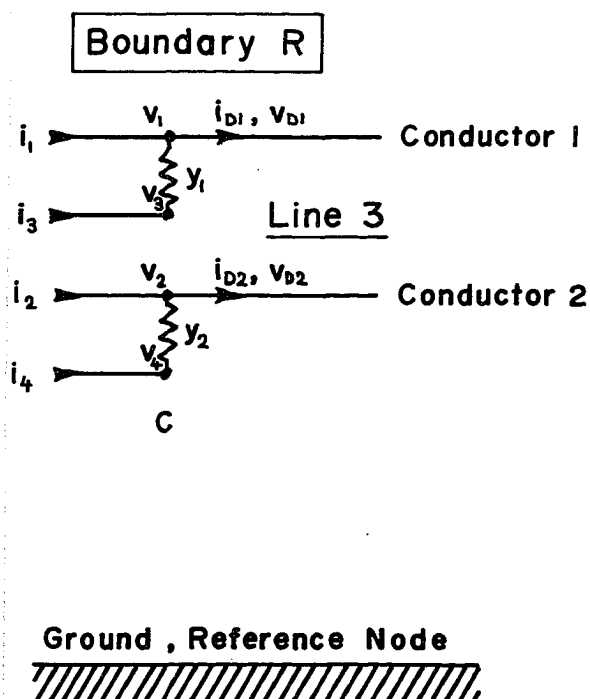


Fig. 3. Nodal Current Network at R.

$$\begin{bmatrix} v_1 \\ v_2 \\ \text{---} \\ v_3 \\ v_4 \end{bmatrix} = \begin{bmatrix} v_\ell \\ \text{---} \\ v_s \end{bmatrix} ; \begin{bmatrix} i_1 \\ i_2 \\ \text{---} \\ i_3 \\ i_4 \end{bmatrix} = \begin{bmatrix} i_\ell \\ \text{---} \\ i_s \end{bmatrix} \quad (5)$$

In a general case, v_ℓ , v_s , i_ℓ , i_s are column vector submatrices with n components. For convenience, the matrix symbols are omitted.

The equations for Line 3 are:

$$\begin{bmatrix} i_{D1} \\ i_{D2} \end{bmatrix} = \begin{bmatrix} Y_{11}^{(3)}, Y_{12}^{(3)} \\ Y_{21}^{(3)}, Y_{22}^{(3)} \end{bmatrix} \begin{bmatrix} v_{D1} \\ v_{D2} \end{bmatrix} \quad \text{or: } i_D = Y_3 v_D \quad (6)$$

The superscript in brackets identifies the entries of the Line 3 admittance matrix. The continuity of voltages on main conductors, Figure 3, requires that

$$v_D = Y_3^{-1} i_D = Z_3 i_D = v_\ell \quad (7)$$

The currents flowing from the stubs into the lumped admittances y_1, y_2 are

$$i_3 = y_1 (v_3 - v_1) \quad (8)$$

$$i_4 = y_2 (v_4 - v_2)$$

or in a matrix form

$$\begin{bmatrix} i_3 \\ i_4 \end{bmatrix} = \begin{bmatrix} y_1 & 0 \\ 0 & y_2 \end{bmatrix} \left\{ \begin{bmatrix} v_3 \\ v_4 \end{bmatrix} - \begin{bmatrix} v_1 \\ v_2 \end{bmatrix} \right\} \quad (9)$$

From (5) and (9), and designating the diagonal matrix by y_ℓ , the general equation is

$$i_s = y_\ell v_s - y_\ell v_\ell \quad (10)$$

The Kirchhoff's law applied to boundary R requires that

$$i_D = i_\ell + i_s = Y_3 v_D = Y_3 v_\ell \quad (11)$$

From (10) and (11)

$$i_\ell = Y_3 v_\ell - i_s = (Y_3 + y_\ell) v_\ell - y_\ell v_s \quad (12)$$

The generalized form of equations (12) and (10) is

$$\begin{bmatrix} i_\ell \\ i_s \end{bmatrix} = \begin{bmatrix} y_\ell + Y_3 & -y_\ell \\ -y_\ell & y_\ell \end{bmatrix} \begin{bmatrix} v_\ell \\ v_s \end{bmatrix} = [y] \begin{bmatrix} v_\ell \\ v_s \end{bmatrix} \quad (13)$$

Equation (13) is the nodal current equation at C. The effective admittance matrix, $[y]$, is a square matrix of the order $2n$ and it is equal to the sum of two matrices.

$$[y] = \begin{bmatrix} y_{\ell} & -y_{\ell} \\ -y_{\ell} & y_{\ell} \end{bmatrix} + \begin{bmatrix} Y_3 & 0 \\ 0 & 0 \end{bmatrix} \quad (14)$$

y_{ℓ} are diagonal submatrices of order n whose elements are equal to the actual admittances that are connected, at the boundary R, between the main conductors and the stubs. Y_3 , also of order n , is the admittance matrix at D of line 3. It is to be noted that the first matrix in equation (14) is singular.

The $2n$ by $2n$ admittance matrix $[y]$, equation (13), can be inverted in a usual way. However, this matrix becomes nearly singular for large values of y_k , and the inversion may produce large errors. Furthermore, although $y_k \rightarrow \infty$ for stubs directly connected to main conductors, the inverse $[y]^{-1} = [z]$ may exist. To overcome the difficulty, matrix $[y]$, equation (13), is partitioned and, because of its particular form, the inversion can be considerably simplified and become more precise. In effect, the inversion of the $2n$ by $2n$ matrix reduces to the inversion of the n by n submatrices y_{ℓ} (diagonal), and Y_3 . From equation (11)

$$v_{\ell} = Y_3^{-1} (i_{\ell} + i_s) = Z_3 (i_{\ell} + i_s) \quad (15)$$

From (15) and (10)

$$i_s = y_{\ell} v_s - y_{\ell} Z_3 i_{\ell} - y_{\ell} Z_3 i_s \quad (16)$$

From (15) and the rearranged equation (16) after premultiplication by y_ℓ^{-1}

$$\begin{bmatrix} v_\ell \\ v_s \end{bmatrix} = \begin{bmatrix} z_3 & z_3 \\ z_3 & z_3 + y_\ell^{-1} \end{bmatrix} \begin{bmatrix} i_\ell \\ i_s \end{bmatrix} = [y]^{-1} \begin{bmatrix} i_\ell \\ i_s \end{bmatrix} \quad (17)$$

Hence, the effective termination impedance matrix

$$[z] = [y]^{-1} = \begin{bmatrix} z_3 & z_3 \\ z_3 & z_3 + z_\ell \end{bmatrix} \quad (18)$$

The impedance matrix $[z]$ can, therefore, be directly obtained by adding up two matrices composed of the inverses of elementary submatrices:

$$[z] = [y]^{-1} = \begin{bmatrix} z_3 & z_3 \\ z_3 & z_3 \end{bmatrix} + \begin{bmatrix} 0 & 0 \\ 0 & z_\ell \end{bmatrix} \quad (19)$$

where $z_3 = Y_3^{-1}$, and z_ℓ is a diagonal matrix whose n elements are the actual impedances connected between the main conductors and the stubs.

In the extreme case of stubs directly connected to the main conductors at C, the termination impedance matrix becomes

$$[z_0] = \begin{bmatrix} z_3 & z_3 \\ z_3 & z_3 \end{bmatrix} \quad (20)$$

This matrix is singular. The subscript 0 indicates that the stubs are connected to the main conductors through zero impedance circuits. Hence, for this case, equation (17) becomes

$$\begin{bmatrix} v_l \\ v_s \end{bmatrix} = \begin{bmatrix} z_o \end{bmatrix} \begin{bmatrix} i_l \\ i_s \end{bmatrix} \quad (21)$$

In this section, equations were developed to find the voltages or currents of Line 3, after the filter, in terms of currents or voltages of Line 2, equations (17) and (13), respectively. These equations are valid for finite values of admittances or impedances of the networks connected between the main conductors and the stubs at boundary R. For the stubs directly connected to the main conductors equation (21) must be used.

The voltages and currents at B and C are related by the generalized equations with a, b, c, d matrix constants³ for length L of Line 2. Referring to Figure 2, these equations are

$$\begin{bmatrix} v_B \\ v_s \end{bmatrix} = \begin{bmatrix} v_l \\ v_s \end{bmatrix} = a \begin{bmatrix} v_l \\ v_s \end{bmatrix} + b \begin{bmatrix} i_l \\ i_s \end{bmatrix} \quad (22)$$

$$\begin{bmatrix} I_B \\ I_s \end{bmatrix} = \begin{bmatrix} I_l \\ I_s \end{bmatrix} = c \begin{bmatrix} v_l \\ v_s \end{bmatrix} + d \begin{bmatrix} i_l \\ i_s \end{bmatrix} \quad (23)$$

where for a Lossless Line, (assumption 1 p.2)

$$a = d = \cos \beta L [1] ; \quad b = j \sin \beta L [Z_2] ; \quad c = j \sin \beta L [Y_2] \quad (24)$$

$[1]$ in equation (24) is the unit matrix, and $[Z_2]$ and, $[Y_2] = [Z_2]^{-1}$ are surge impedance and admittance matrices of Line 2, respectively.

Designating by f_0 the principal resonance frequency at which L is equal to a quarter wavelength, the value of βL in (24) at frequency f is

$$\beta L = \frac{\pi f}{2 f_0} \quad (25)$$

Since the total number of conductors in Line 2 is $2n$, the unit matrix, and the surge impedance and admittance matrices of Line 2 are of order $2n$. Equations (22) and (23) become similar to a single-conductor line a, b, c - constants equations if new symbols without matrix notation are introduced.

$$V = av + bi \quad (26)$$

$$I = cv + ai \quad (27)$$

where

$$V = \begin{bmatrix} V_B \\ V_S \end{bmatrix} = \begin{bmatrix} v_\ell \\ v_s \end{bmatrix} ; \quad I = \begin{bmatrix} I_B \\ I_S \end{bmatrix} = \begin{bmatrix} I_\ell \\ I_s \end{bmatrix} \quad (28)$$

$$v = \begin{bmatrix} v_c \end{bmatrix} = \begin{bmatrix} v_\ell \\ v_s \end{bmatrix} ; \quad i = \begin{bmatrix} i_c \end{bmatrix} = \begin{bmatrix} i_\ell \\ i_s \end{bmatrix} \quad (29)$$

The alternate form of equations (26) and (27) is

$$v = aV - bI \quad (30)$$

$$i = -cV + aI \quad (31)$$

Introducing the simplified notation, equations (28) and (29), to

equations (13), (14), (17) and (18), the R-boundary equations are found:

$$i = yv \quad (32)$$

$$v = y^{-1}i = zi \quad (33)$$

From equations (26) to (33) the voltages or currents of Line 3 at D, Figure 2, can be directly related to the currents or voltages at B. Furthermore, the input admittance matrix, Y_B , and its inverse, Z_B , are derived in various forms.

Eliminating v or i in equations (26) and (27) by substituting (32) or (33)

$$v = (a + by)^{-1}v \quad (34)$$

$$v = (c + ay)^{-1}I \quad (35)$$

$$i = (b + az)^{-1}v \quad (36)$$

$$i = (a + cz)^{-1}I \quad (37)$$

Substituting equations (30) and (31) in (32) or (33), and performing matrix premultiplication

$$I = Y_B V \quad (38)$$

where Y_B can be expressed by any of the following equations

$$Y_B = (a + yb)^{-1}(c + ya) \quad (39)$$

$$Y_B = (c + ay)(a + by)^{-1} \quad (40)$$

$$Y_B = (b + za)^{-1} (a + zc) \quad (41)$$

$$Y_B = (a + cz) (b + az)^{-1} \quad (42)$$

Equations (39) to (42) are the matrix admittances, Y_B , of a filter open ended at boundary T, for $Y_\ell = 0$. The inverse of Y_B is equal to the input impedance of the filter at B. For example, from equation (42)

$$Z_B = Y_B^{-1} = (b + az) (a + cz)^{-1} \quad (43)$$

For a finite termination at T, the total input admittance matrix Y is equal to the sum of the admittance matrix of the terminating networks Y_T and Y_B . Hence, similarly to equation (14)

$$Y = Y_T + Y_B \quad (44)$$

Referring to Figures (1) and (2), (pp. 1 and 5),

$$Y_T = \begin{bmatrix} Y_\ell & -Y_\ell \\ -Y_\ell & Y_\ell \end{bmatrix} \quad (45)$$

where Y_ℓ is a diagonal submatrix whose elements are the actual admittances of \wedge the \wedge networks \wedge connected between the main conductors and the corresponding stubs at boundary T

$$Y_\ell = \begin{bmatrix} Y_1 & 0 & \text{-----} & 0 \\ 0 & Y_2 & \text{-----} & 0 \\ \vdots & & & \vdots \\ \vdots & & & \vdots \\ \vdots & & & \vdots \\ 0 & \text{-----} & \text{-----} & Y_n \end{bmatrix} \quad (46)$$

The filter looked at from the Line 1 side can be considered as a multinode network whose input admittance ^{matrix} is Y , equation (44). This matrix of order $2n$, when partitioned into submatrices of order n , is

$$Y = \begin{bmatrix} Y_{ll} & \vdots & Y_{ls} \\ \text{---} & \vdots & \text{---} \\ Y_{sl} & \vdots & Y_{ss} \end{bmatrix} \quad (47)$$

The nodal currents injected into this multinode network are only the n conductor current components of I_A , flowing from Line 1. No currents are injected into the nodes representing the junction of the n stubs and terminating impedances Y_{ℓ} , equation (46). Hence, the nodal current equation is

$$\begin{bmatrix} I_A \\ 0 \end{bmatrix} = \begin{bmatrix} Y_{ll} & Y_{ls} \\ Y_{sl} & Y_{ss} \end{bmatrix} \begin{bmatrix} V_{\ell} \\ V_s \end{bmatrix} \quad (48)$$

Because of the continuity of voltages on the main conductors, V_{ℓ} components are equal to the conductor components V_A of Line 1, Figure 2, (p.5),

$$V_{\ell} = V_A \quad (49)$$

Premultiplying equation (48) by the inverse of Y , equation (47),

$$Y^{-1} = Z = \begin{bmatrix} Z_{ll} & Z_{ls} \\ Z_{sl} & Z_{ss} \end{bmatrix} \quad (50)$$

$$\begin{bmatrix} v_l \\ v_s \end{bmatrix} = \begin{bmatrix} z_{ll} & z_{ls} \\ z_{sl} & z_{ss} \end{bmatrix} \begin{bmatrix} I_A \\ 0 \end{bmatrix} \quad (51)$$

From equations (51) and (49)

$$v_l = v_A = z_{ll} I_A \quad (52)$$

$$v_s = z_{sl} z_{ll}^{-1} v_A \quad (53)$$

It must be noted that z_{ll} , z_{sl} are not the inverses of submatrices Y_{ll} and Y_{sl} in equation (47).

There are several ways to find the Line 3 voltages, v_D , in terms of the Line 1 voltages, v_A , with the aid of the various equations already developed.

For example, from equations (28), (29), (34), (52) and (53), and $v_l = v_D$

$$\begin{bmatrix} v_l \\ v_s \end{bmatrix} = \begin{bmatrix} (a + by)^{-1} \end{bmatrix} \begin{bmatrix} v_l \\ v_s \end{bmatrix} = [P] \begin{bmatrix} v_l \\ v_s \end{bmatrix} = \begin{bmatrix} v_D \\ v_s \end{bmatrix} = [P] \begin{bmatrix} v_A \\ z_{sl} z_{ll}^{-1} v_A \end{bmatrix} \quad (54)$$

Again, partitioning $[P]$ and solving for v_D

$$[P] = (a + by)^{-1} = \begin{bmatrix} P_{ll} & P_{ls} \\ P_{sl} & P_{ss} \end{bmatrix} \quad (55)$$

$$v_D = (P_{ll} + P_{ls} z_{sl} z_{ll}^{-1}) v_A \quad (56)$$

Equations such as (56) allow the Line 3 conductor voltages, v_D , to be calculated for any set of Line 1 voltages, V_A , at the filter input.

In the next step of the analysis equations for conductor voltages V'_A at the junction of Line 3 that is directly connected to Line 1 are developed. V_A in equation (56) will be expressed in terms of V'_A and thus the attenuating properties of the filter can be assessed.

Evaluation of Attenuation

In order to assess the effect of the filter inserted between two lines, two cases are considered. In the first instance, Line 3 is extended to point A of Line 1, Figure 2, (p.1),

Let the impedance matrices when looking into Line 1 and into the extended Line 3 be Z_1 and Z_{3e} respectively. Let the terminal voltages of Line 1 when open ended at A be V_{Aoc} . Applying the Thevenin's theorem the currents I'_A flowing into Line 3 are defined by

$$I'_A = (Z_1 + Z_{3e})^{-1} V_{Aoc} \quad (57)$$

and, hence, the voltage V'_A at A is

$$V'_A = Z_{3e} I'_A = Z_{3e} (Z_1 + Z_{3e})^{-1} V_{Aoc} \quad (58)$$

Solving (58) for V_{Aoc} and simplifying

$$V_{Aoc} = (Z_1 Z_{3e}^{-1} + 1) V'_A \quad (59)$$

where 1 is the unit matrix of order n.

Similarly, the corresponding equations for the filter connected at A are

$$I_A = (Z_1 + Z_f)^{-1} V_{Aoc} \quad (60)$$

$$V_A = Z_f I_A \quad (61)$$

$$V_{Aoc} = (Z_1 Z_f^{-1} + 1) V_A \quad (62)$$

where Z_f is the input impedance of the filter.

From equations (59) and (62)

$$V_A = (Z_1 Z_f^{-1} + 1)^{-1} (Z_1 Z_{3e}^{-1} + 1) V'_A \quad (63)$$

The input impedance of the filter, Z_f , is found from equations (52), (51) and (61)

$$V_A = V_\ell = Z_{\ell\ell} I_a = Z_f I_A \quad (64)$$

therefore,

$$Z_f = Z_{\ell\ell} \quad (65)$$

Substituting equation (65) in (63), and the resulting equation in (56)

$$V_D = (P_{\ell\ell} + P_{\ell s} Z_{s\ell} Z_{\ell\ell}^{-1}) (Z_1 Z_{\ell\ell}^{-1} + 1)^{-1} (Z_1 Z_{3e}^{-1} + 1) V'_A \quad (66)$$

Equation (66) is a complete solution of the Q-W filter response at any frequency.

V'_A components are the conductor voltages at A, in the absence of the filter, or the voltages that would exist at the input of the extended Line 3. The conductor components of v_D are the

voltages at the input of Line 3 in the presence of the filter. The effect of the filter can, therefore, be assessed from equation (66) for any values of V_A' conductor voltage components.

In the developing of equation (66) no assumptions were made with respect to Line 1 and Line 3 impedances. Z_3 in equation (7) relates the conductor voltages and currents at the input of Line 3 after the filter. Line 3 does not need to be a reflection-free line. The same applies to Z_{3e} and Z_1 impedance matrices in equation (57). Equation (66) is, therefore, most general for any single filter that may be one of many staggered filters along the line. These filters may be separated by a finite length of line of n conductors. For such a line section without filters the a, b, c, d matrix constants equations (22) and (23), apply directly but the matrices are reduced to order n . A successive application of equations (66) and, if needed, equations (22) and (23), will allow the frequency response of a system of staggered filters to be determined.

It is to be noted that the concept of "attenuation" as a ratio of voltages or powers has a conventional meaning for a filter on a single-phase line only. For multiconductor lines the "attenuation" on one conductor may be different from that on another conductor. This attenuation depends in principle on all conductor components of the input voltage and on the characteristics of each elementary single-stub filter. The resulting square matrix to the left of V_A' in equation (66) contains off-diagonal entries or mutual coupling elements and it is not a conventional attenuation coefficient.

Equation (66) is valid for real or complex terminations at either end of the stubs. For a capacitive termination at the high-impedance end of the filter or an inductive termination at the low impedance end, the resonance frequency f_0 is reduced. Hence, the final adjustment of the peak frequency can be achieved without a change of the actual length of the stubs, equation (25).

Finally, equations (22) to (24) indicate that the filter operates at all odd harmonics of the principal resonance frequency.

CHAPTER 3
DETAILED METHOD

In the Detailed Method a system of linear equations in terms of incident and reflected voltages and currents is derived. This system of equations is solved for a given set of incident voltage components, V^+ . In order to write the system of equations the following conditions are considered:

At the boundaries T and R, Figure 4.

- a) Voltage continuity on the main conductors
- b) Kirchhoff's current law, $\sum I = 0$, at nodes
- c) Ohm's law, $I_{AB} = Y(V_A - V_B)$, for the voltage drop across the admittances.

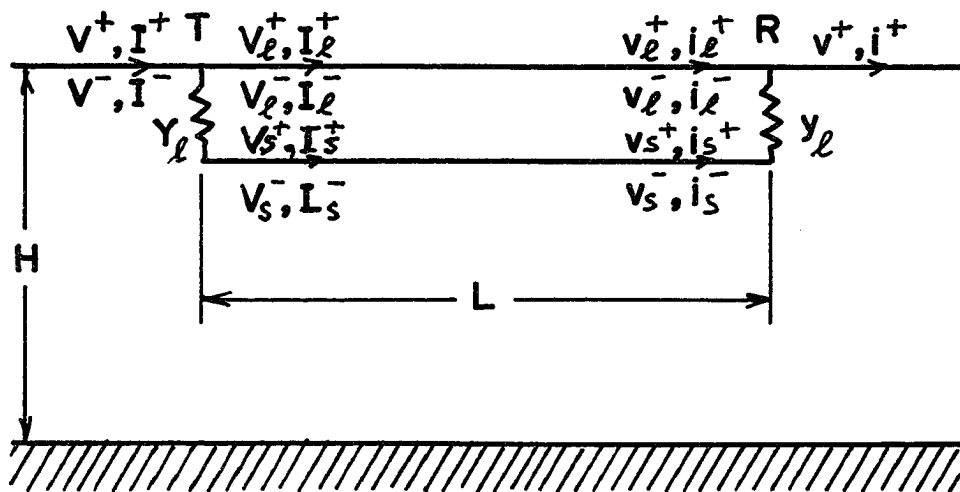


Fig. 4. Diagram of the Reduced System in Figure 1.

On Line 2

- d) The voltage equations on Line 2 between T and R are of the type $V = \epsilon^{-j\beta L} v$, where v is the voltage at a given reference point, V is the voltage at a distance L in the direction of propagation, and $\beta = \frac{\pi}{2} f/f_0$ as in the direct method, equation (25).

On Lines 1, 2 and 3

- e) The current-voltage relations are $I^+ = YV^+$ for waves propagating in the positive direction and $I^- = -YV^-$ for waves propagating in the negative direction, where Y is the surge admittance ^{matrix} of the line.

Boundary conditions a, b and c are used together with general equations (3) and (4):

$$V = V^+ + V^- \quad (3)$$

$$I = I^+ + I^- \quad (4)$$

The solution of the system of these equations yields all voltages, in particular v^+ , at the output of the filter. Line 3 is assumed to be reflection-free, hence $v^- = 0$, and v^+ is therefore the total conductor voltage, v .

Derivation of the Equations

Boundary T

From condition (a)

$$V = V_l$$

$$V^+ + V^- = V_l^+ + V_l^- \quad (67)$$

Condition (b)

$$I - I_\ell - I_s = 0$$

$$(I^+ + I^-) - (I_\ell^+ + I_\ell^-) - (I_s^+ + I_s^-) = 0 \quad (68)$$

Condition (c)

$$I_s = Y_\ell (V_\ell - V_s)$$

$$I_s^+ + I_s^- = Y_\ell [(V_\ell^+ + V_\ell^-) - (V_s^+ + V_s^-)] \quad (69)$$

Boundary_R

From condition (a)

$$V_\ell = V$$

$$V_\ell^+ + V_\ell^- = V^+ \quad (70)$$

Condition (b)

$$i_\ell + i_s - i = 0$$

$$(i_\ell^+ + i_\ell^-) + (i_s^+ + i_s^-) - i^+ = 0 \quad (71)$$

Condition (c)

$$i_s = Y_\ell (V_s - V_\ell)$$

$$i_s^+ + i_s^- = Y_\ell [(V_s^+ + V_s^-) - (V_\ell^+ + V_\ell^-)] \quad (72)$$

On_Line_2

$$\begin{bmatrix} V_\ell^+ \\ V_s^+ \end{bmatrix} = \epsilon^{-j\beta L} \begin{bmatrix} V_\ell^+ \\ V_s^+ \end{bmatrix}$$

$$V_\ell^+ = \epsilon^{-j\beta L} V_\ell^+ \quad (73)$$

$$v_s^+ = e^{-j\beta L} v_s^+ \quad (74)$$

also

$$\begin{bmatrix} v_l^- \\ v_s^- \end{bmatrix} = e^{-j\beta L} \begin{bmatrix} v_l^- \\ v_s^- \end{bmatrix}$$

$$v_l^- = e^{-j\beta L} v_l^- \quad (75)$$

$$v_s^- = e^{-j\beta L} v_s^- \quad (76)$$

On Line 1, 2 and 3

Line 1

$$I^+ = Y_1 V^+ \quad (77)$$

$$I^- = -Y_1 V^- \quad (78)$$

Line 2 at T

$$\begin{bmatrix} I_l^+ \\ I_s^+ \end{bmatrix} = Y_2 \begin{bmatrix} V_l^+ \\ V_s^+ \end{bmatrix} = \begin{bmatrix} Y_{ll} & Y_{ls} \\ Y_{sl} & Y_{ss} \end{bmatrix} \begin{bmatrix} V_l^+ \\ V_s^+ \end{bmatrix}$$

$$I_l^+ = Y_{ll} V_l^+ + Y_{ls} V_s^+ \quad (79)$$

$$I_s^+ = Y_{sl} V_l^+ + Y_{ss} V_s^+ \quad (80)$$

and

$$\begin{bmatrix} I_l^- \\ I_s^- \end{bmatrix} = -Y_2 \begin{bmatrix} V_l^- \\ V_s^- \end{bmatrix}$$

$$I_l^- = -Y_{ll} V_l^- - Y_{ls} V_s^- \quad (81)$$

$$I_s^- = -Y_{sl} v_l^- - Y_{ss} v_s^- \quad (82)$$

Line 2 at R

$$\begin{bmatrix} i_l^+ \\ i_s^+ \end{bmatrix} = Y_2 \begin{bmatrix} v_l^+ \\ v_s^+ \end{bmatrix}$$

$$i_l^+ = Y_{ll} v_l^+ + Y_{ls} v_s^+ \quad (83)$$

$$i_s^+ = Y_{sl} v_l^+ + Y_{ss} v_s^+ \quad (84)$$

$$\begin{bmatrix} i_l^- \\ i_s^- \end{bmatrix} = -Y_2 \begin{bmatrix} v_l^- \\ v_s^- \end{bmatrix}$$

$$i_l^- = -Y_{ll} v_l^- - Y_{ls} v_s^- \quad (85)$$

$$i_s^- = -Y_{sl} v_l^- - Y_{ss} v_s^- \quad (86)$$

Line 3

$$i^+ = Y_3 v^+ \quad (87)$$

Equations (67) to (87) represent a system of 21 simultaneous linear matrix equations. It is to be noted that V and Y are matrices,

$$V = \begin{bmatrix} v_1 \\ \cdot \\ \cdot \\ \cdot \\ v_N \end{bmatrix}; \quad v^+ = \begin{bmatrix} v_1^+ \\ \cdot \\ \cdot \\ \cdot \\ v_N^+ \end{bmatrix}; \quad v^- = \begin{bmatrix} v_1^- \\ \cdot \\ \cdot \\ \cdot \\ v_N^- \end{bmatrix}; \quad \text{etc.}$$

and

$$Y = \begin{bmatrix} Y_{11} & Y_{12} & \cdot & \cdot & \cdot & \cdot & Y_{1N} \\ \cdot & & & & & & \\ \cdot & & & & & & \\ \cdot & & & & & & \\ Y_{N1} & \cdot & \cdot & \cdot & \cdot & \cdot & \cdot Y_{NN} \end{bmatrix}$$

The system of these 21 fundamental matrix equations can be solved for a set of given incident voltage components V^+ . This system can be reduced to 10 matrix equations by eliminating the current vector matrices in the following manner.

Combining equations (77) to (82) with equation (68),

$$\begin{aligned} Y_1 V^+ - Y_1 V^- - (Y_{ll} + Y_{sl}) V_l^+ + (Y_{ll} + Y_{sl}) V_l^- - \\ - (Y_{ls} + Y_{ss}) V_s^+ + (Y_{ls} + Y_{ss}) V_s^- = 0 \quad , \end{aligned} \quad (88)$$

equations (80) and (82) with equation (69)

$$(Y_{sl} - Y_l) V_l^+ - (Y_{sl} + Y_l) V_l^- + (Y_{ss} + Y_l) V_s^+ - (Y_{ss} + Y_l) V_s^- = 0 \quad (89)$$

Combining equations (83) to (87) with equation (71)

$$\begin{aligned} (Y_{ll} + Y_{sl}) V_l^+ - (Y_{ll} + Y_{sl}) V_l^- + (Y_{ls} + Y_{ss}) V_s^+ - (Y_{ls} + Y_{ss}) V_s^- - \\ - Y_3 V^+ = 0 \quad , \end{aligned} \quad (90)$$

equations (84) and (86) with equation (72)

$$(Y_{sl} + y_l) V_l^+ - (Y_{sl} - y_l) V_l^- + (Y_{ss} - y_l) V_s^+ - (Y_{ss} + y_l) V_s^- = 0 \quad (91)$$

Equations (67), (70), (73) to (76), and (88) to (91) form the reduced system of 10 matrix equations.

that

It should be noted ^{that} the system of equivalent scalar equations consists of $10N$ equations, where N is the number of main conductors.

The system of matrix equations can be written in ^{the} simplified notation.

$$AX = B, \quad (92)$$

where

$$X = \begin{bmatrix} v_{\ell}^+ \\ v_{\ell}^- \\ v_s^+ \\ v_s^- \\ v_{\ell}^+ \\ v_{\ell}^- \\ v_s^+ \\ v_s^- \\ v^- \\ v^+ \end{bmatrix} \quad B = \begin{bmatrix} v^+ \\ 0 \\ 0 \\ 0 \\ 0 \\ 0 \\ Y_1 v^+ \\ 0 \\ 0 \\ 0 \end{bmatrix}$$

and the matrix A is given on the following page. In the matrix A , U is the n^{th} order unit matrix.

Premultiplying (92) by A^{-1}

$$X = A^{-1} B \quad (93)$$

The attenuation of the filter in dB is

$$b_f = 20 \log_{10} \left(\frac{v^+}{v^+} \right) \quad (\text{dB}) \quad (94)$$

This equation is valid for identical and reflection-free Lines 1 and 3.

A=

U				
$-\epsilon^{-j\beta L}$				U
		$-\epsilon^{-j\beta L}$		U
	U			
			U	
$Y_{ll} + Y_{sl}$	$-(Y_{ll} + Y_{sl})$	$Y_{ls} + Y_{ss}$	$-(Y_{ls} + Y_{ss})$	
$Y_{sl} - Y_l$	$-(Y_{sl} + Y_l)$	$Y_{ss} + Y_l$	$-(Y_{ss} + Y_l)$	
				$Y_{ll} + Y_{sl}$
				$Y_{sl} + Y_l$

			$-U$	
U				$-U$
	U			
$-\epsilon^{-j\beta L}$				
		$-\epsilon^{-j\beta L}$		
			Y_l	
$-(Y_{ll} + Y_{sl})$	$Y_{ls} + Y_{ss}$	$-(Y_{ls} + Y_{ss})$		$-Y_3$
$-(Y_{sl} - Y_l)$	$Y_{ss} - Y_l$	$-(Y_{ss} + Y_l)$		

In a general case, Lines 1 and 3 may be not identical and reflections may exist at the far end of these lines. In this instance a system of 19 matrix equations is written in terms of the wave quantities on Line 2, and the filter terminal quantities V , I , v and i . This system can also be reduced to 10 equations by eliminating all currents except I , at the input of the filter. The solution of the reduced system will, among others, yield the important relation between the filter output voltage v in terms of V at the filter input. In order to assess the attenuation properties of the filter the analysis proceeds along the same lines as in the Direct Method.

CHAPTER 4

THE SAWADA AND NAKAMURA METHOD.

COMPARISON BETWEEN CALCULATED AND EXPERIMENTAL RESULTS.

The Sawada and Nakamura Method

The analysis developed by Sawada and Nakamura considers a *conductor* single line isolated in space with N stubs placed around the main conductor. The stubs are open-ended at one extremity and connected through a resistance to the main conductor at the other end.

Figure 5 represents such an arrangement for $N = 1$.

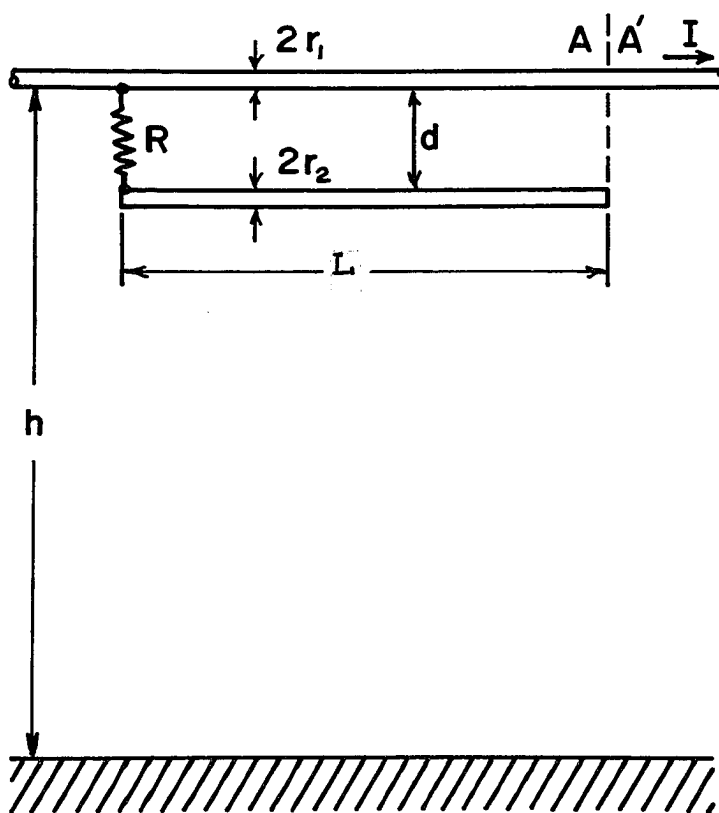


Fig. 5. Q-W Filter by Sawada and Nakamura¹.

The high frequency current I is resolved into positive (line-to-stub) and zero sequence (line-to-ground) components. This resolution led the authors to derive an equivalent circuit in which the filter acts as a series impedance $k^2 Z_b$, where k depends on N , the radii r_1 and r_2 , and the spacing d between the stub and the line conductor.

The assumption by the authors that the filter can be represented by an impedance in series with the line greatly simplifies the analysis. Figure 6 illustrates the principle for a system where $N = 1$ and $r_1 = r_2$.

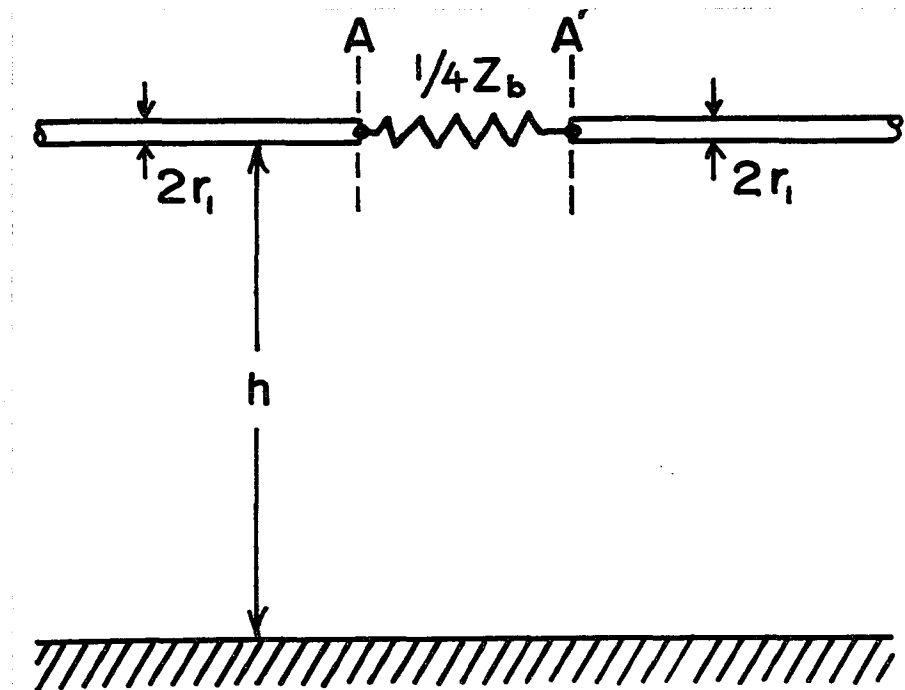


Fig. 6. Equivalent Circuit of Line and Filter
in Figure 5.

Neglecting line losses ($\alpha=0$), the following equation for the filter attenuation is derived from Figure 6.

$$b_f = 20 \log_{10} \left[1 + \frac{Z_b}{8Z_o} \right] \text{ (dB)} \quad (95)$$

where

$$Z_b = Z_1 \frac{R + jZ_1 \operatorname{tg} \beta L}{Z_1 + jR \operatorname{tg} \beta L} \quad (96)$$

$$Z_1 = 120 \operatorname{Ln} \frac{d}{r_1} \quad (97)$$

$$Z_o = 60 \operatorname{Ln} \frac{2h}{r_1} \quad (98)$$

Z_1 is the surge impedance of a two-conductor line isolated in space, and Z_o is the surge impedance of the single-conductor line to the left and the right of the filter.

Experimental Results

Sawada and Nakamura studied the performance of the quarter-wave filter on the experimental model line shown in Figure 7.

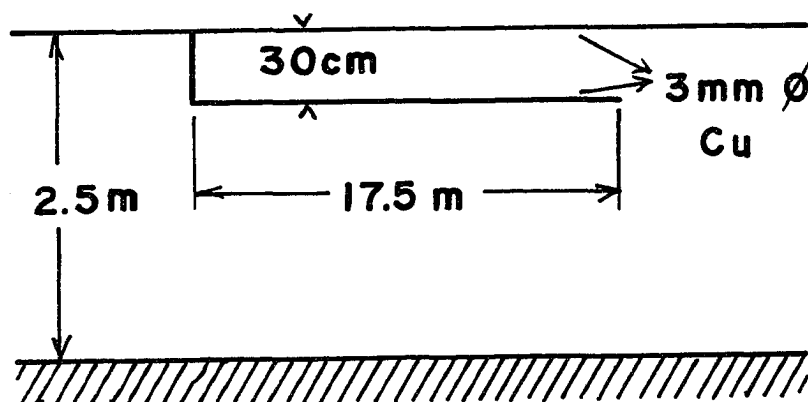


Fig. 7. Model Line used by Sawada and Nakamura.

The effect on filter performance of resistive and capacitive filter terminations, stub spacing and stub conductor radius were evaluated. Also the effect of cascading several filters was demonstrated. The test frequency was in the MHz range.

Figure 8 shows the experimental curve obtained by Sawada and Nakamura on the model line of Figure 7, for the filter short-circuited at one end and open-circuited at the other. The centre test frequency was 4.2 MHz.

Figure 8, the calculated frequency response curve, was obtained using the analysis developed in this thesis. An examination of the response curves shows a good agreement between experimental and calculated results; particularly in the useful range above 6dB.

Dr. M. Ushirozawa communicated to us his results of a quarter-wave filter shown in Figure 9.

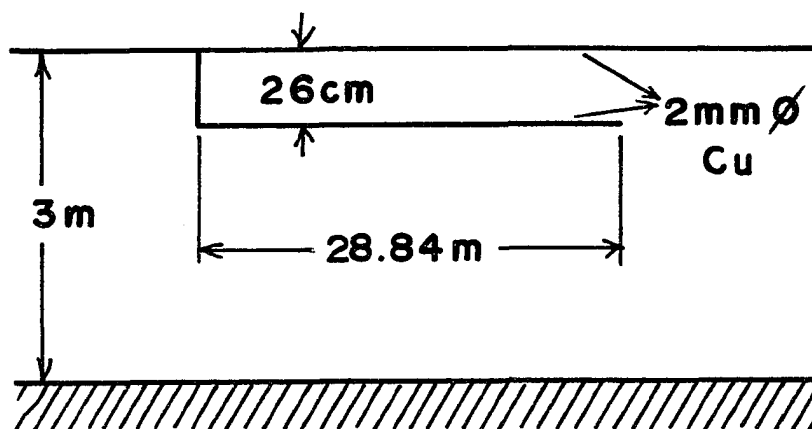


Fig. 9. Model Line used by Dr. M. Ushirozawa.

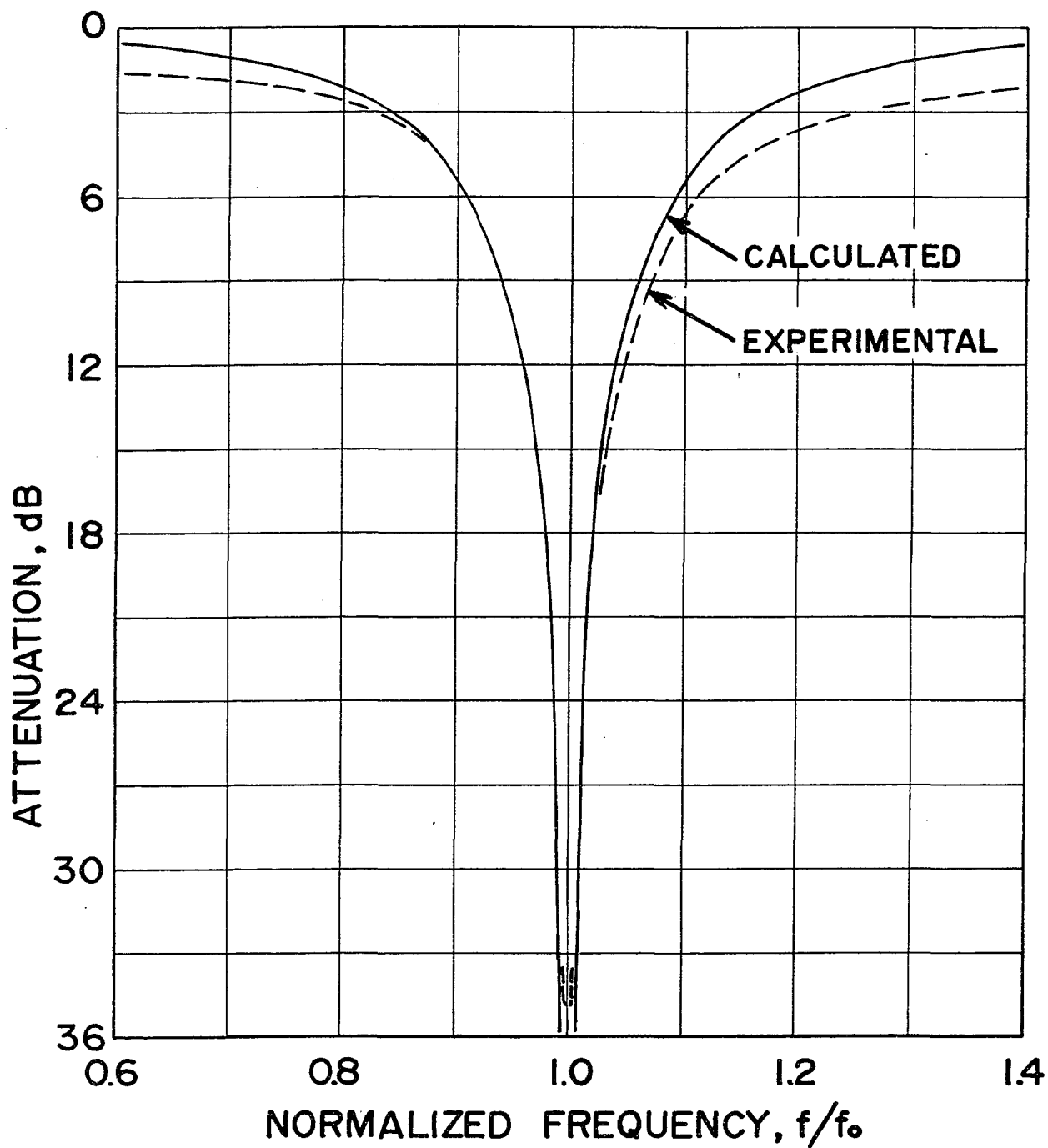


Fig. 8. Experimental (Sawada and Nakamura) and calculated (Thesis) frequency response.

Again the calculated and experimental curves illustrated in Figure 10 are in good agreement.

The experimental and calculated results in Figures 8 and 10 indicate that for 6dB and 12dB the band-widths are about 18% and 8%, respectively, for both model lines. This can be explained by the similarity of the test lines.

The experimental results obtained on single line models were ^{found} so encouraging that quarter-wave filters were installed on the double circuit, three phase, 250 kV, Itami-Himeji power line. Attenuations better than 30 dB were measured at 940 KHz and 1,150 KHz. The operation of this filter over a period of two years was found very satisfactory.

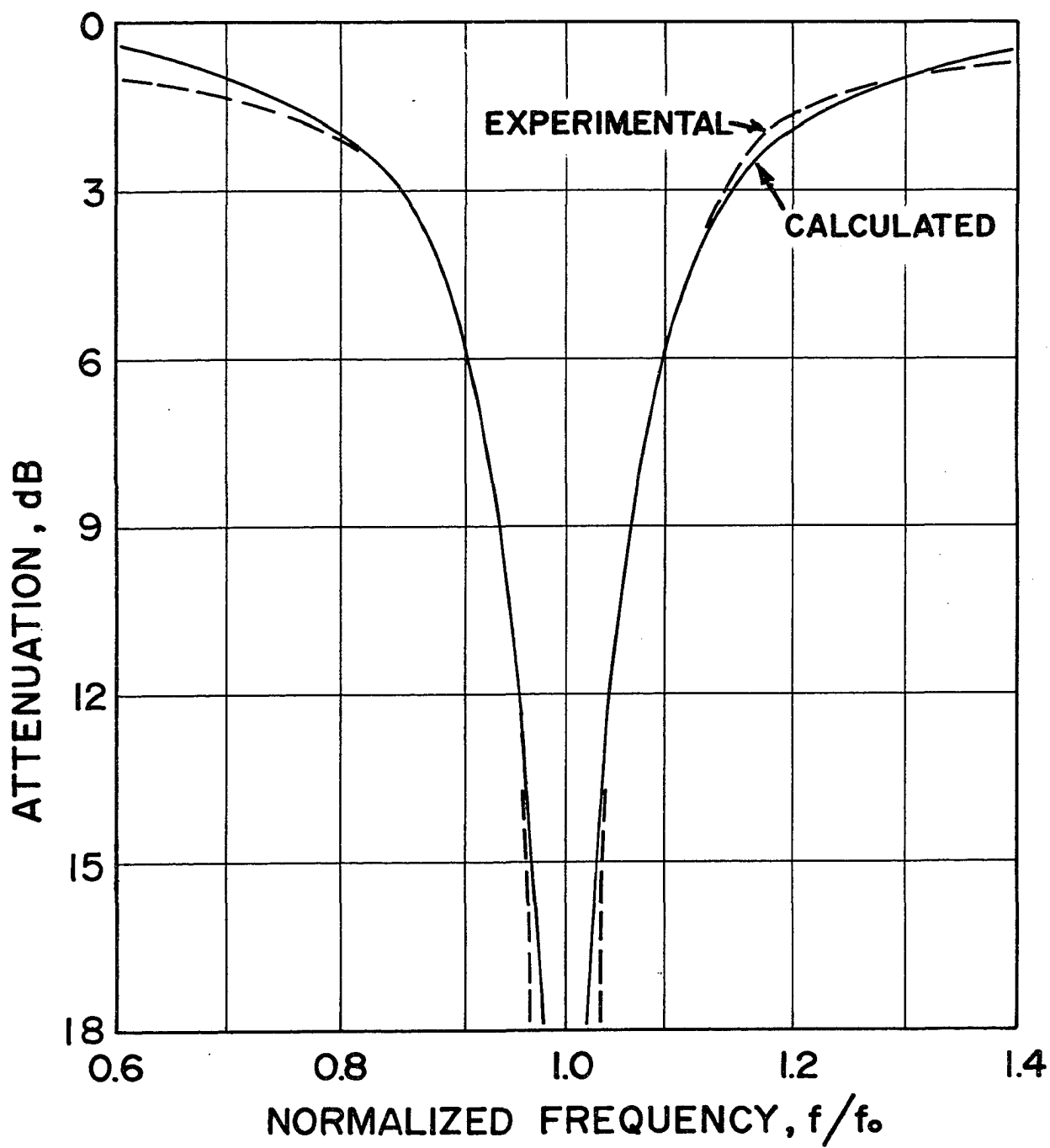


Fig. 10. Experimental (Dr. M. Ushirozawa) and calculated (Thesis) frequency response curves.

CHAPTER 5

FILTER PERFORMANCE ON FULL SCALE LINES

This chapter presents the results of the calculations using the Direct and the Detailed Methods. Both methods were applied to a line with a geometry similar to that of a conventional power line.

At first, the effect of filter termination and filter geometry is studied for a single phase line. Next, filters on two and three ^{horizontal} phase lines are analyzed.

The line dimensions are:

Line height	$h = 40$ ft
Conductor diameter	$2r = 1.5$ in
Spacing between adjacent phases	40 ft

Single Phase Line

Effect of termination on frequency response

To study the effect of termination, a stub spacing of 18 in. and stub conductor size, 1.5 in. were used in all calculations.

Figure 11 shows the frequency response curves for a filter open-ended at T and terminated with a resistance at R (Fig. 4). The values of termination resistances for the three curves are as *marked*. It is seen that the response curve between 6dB and 12dB does not change much when the resistance at R is increased from $10^{-3} \Omega$ to 10Ω . However, the attenuation at the resonance frequency f_0 changes drastically. Hence, it may be concluded that as long as the terminating resistance of the filter open-

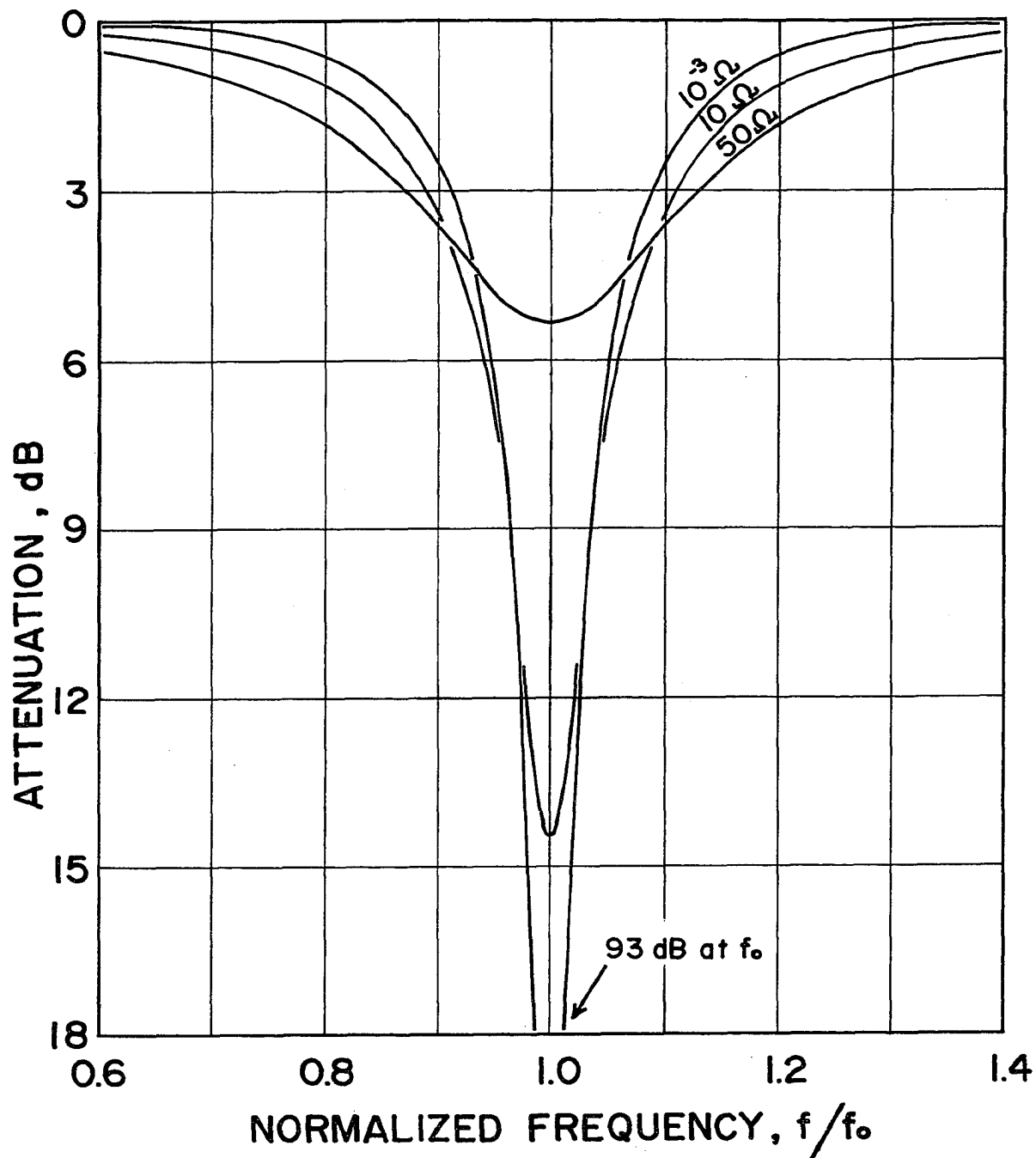


Fig. 11. Calculated Frequency Response Curves for Resistive Terminations at R, Figure 2, 10^{-3} Ohms, 10 Ohms and 50 Ohms.

ended at one end is small, the frequency response changes little within the practical range of attenuation. The same conclusion could have been made from Figure 12, where the bandwidths at different attenuation levels are plotted versus termination resistances at R or T. The scale of the lower abscissa is, approximately, inversely proportional to R_T for the filter shorted at R, Figure 4.

Examination of Figure 12 also reveals that, for any desired attenuation, the value of the termination resistance for maximum bandwidth is not critical.

To study a capacitive tuning arrangement, a capacitor C_T in parallel with a $10\text{ K}\Omega$ resistor at T and a short ($10^{-3}\Omega$) at R was used.

Figure 13 shows the frequency response curves for different values of capacitance. It can be observed that as the capacitance increases:

- the peak attenuation frequency is reduced
- the maximum attenuation does not change appreciably
- the bandwidth reduces, and
- the attenuation curve loses its symmetry.

The peak attenuation frequency $f_{r,\lambda}$ ^{the} bandwidth in percent of the original resonance frequency f_o , and the bandwidth in percent of the new resonance frequency f_r , versus the logarithm of C_T are plotted in Figure 14.

It can be concluded from an examination of these graphs that a given filter can be used at lower frequencies without changing the length of the stubs but at the expense of reducing

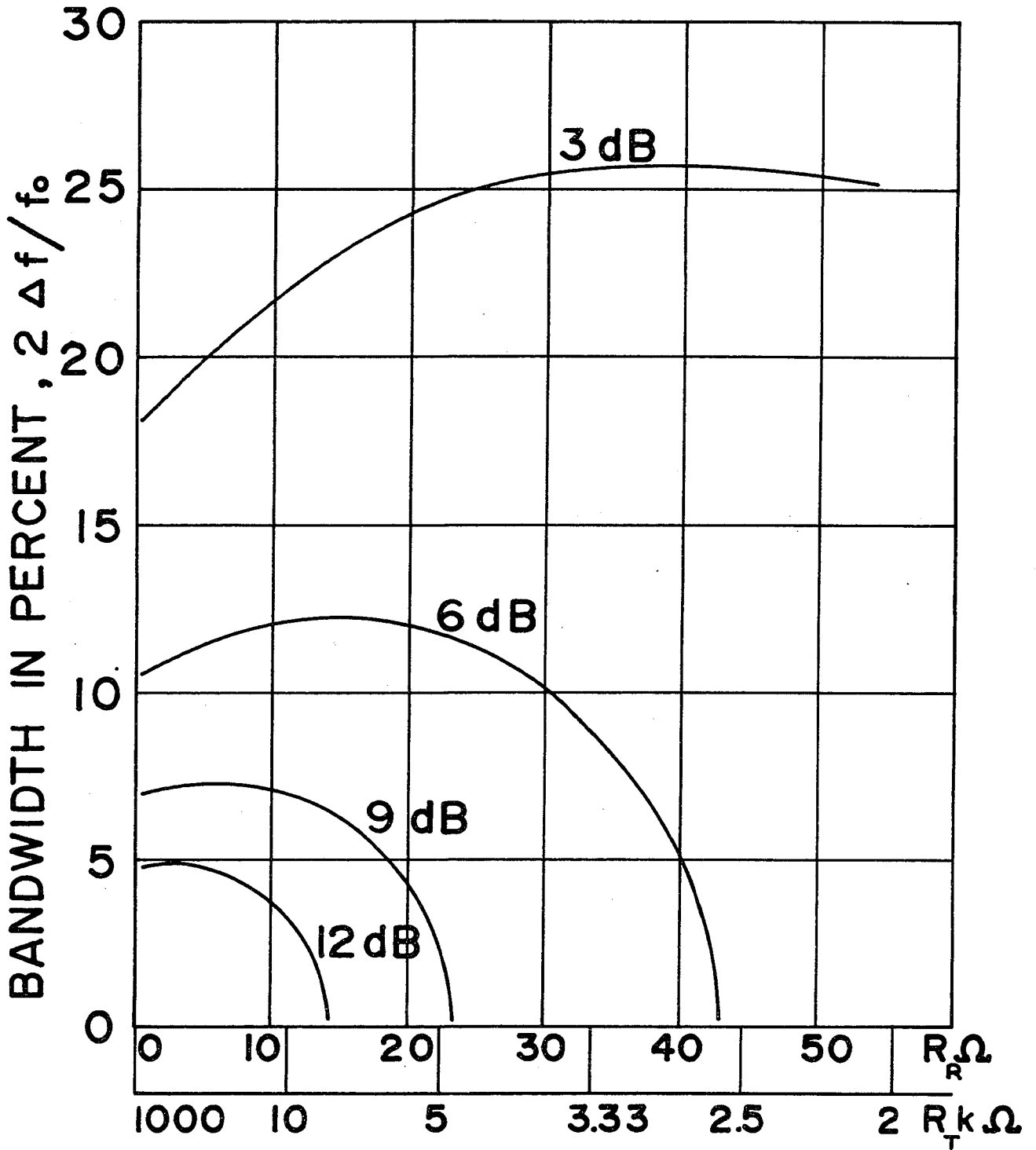


Fig. 12. Bandwidth, $2\Delta f/f_0$, in Percent as a Function of Resistive Terminations, R_R and R_T , at R and T, Figure 2.

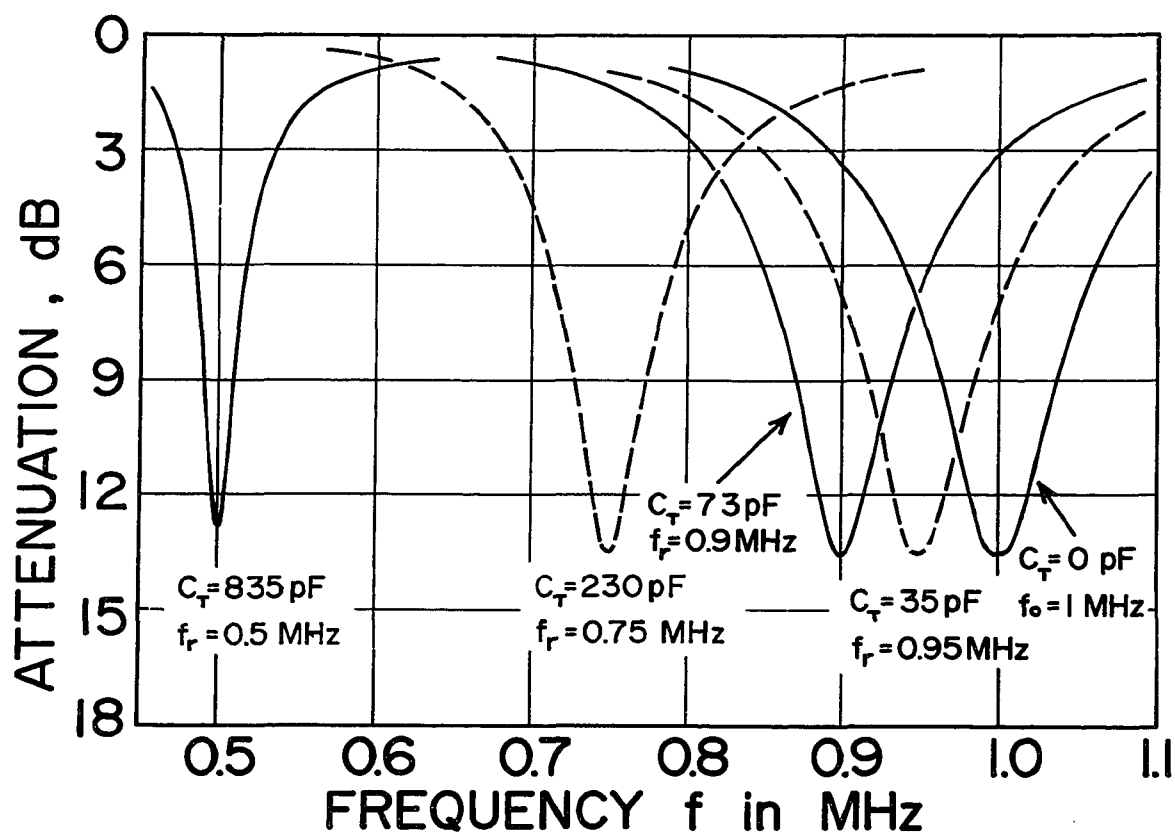


Fig. 13. Frequency Response Curves for Capacitive Termination.

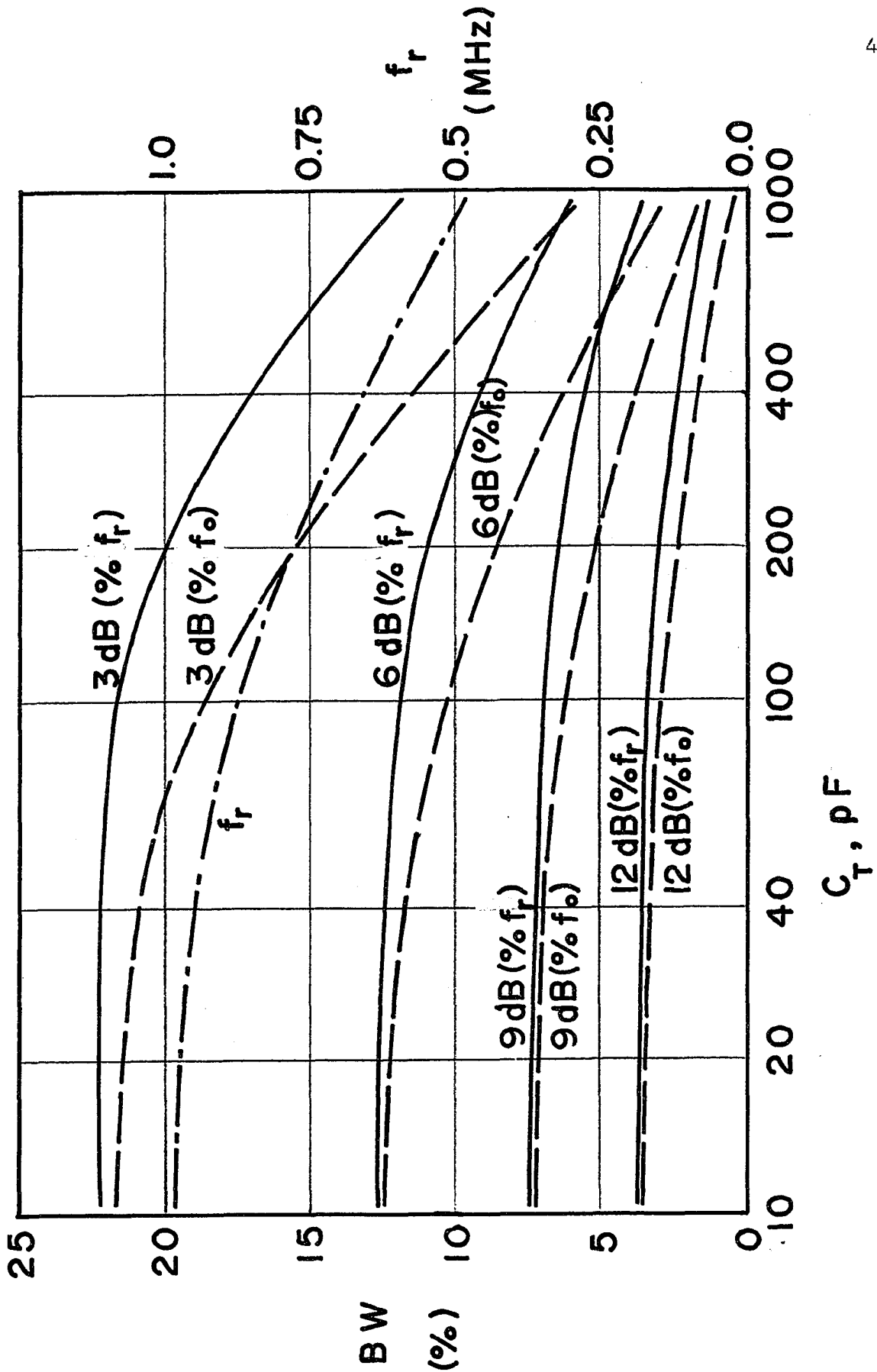


Fig. 14. Effect of Capacitance C_T on the Resonance Frequency f_r and the Bandwidth.

the bandwidth. For example, if the peak frequency is reduced from its original value of 1 MHz to 750 KHz by adding the capacitance $C_T = 230 \text{ pF}$ the bandwidth at the 6dB level changes from 125 KHz to 80 KHz. A method is presented in Appendix B how to calculate the capacitance necessary for a given shift of the peak frequency.

Effect of Filter Geometry

In the previous section the effect of termination on the filter performance was studied while the stub spacing and conductor size were held constant. This section considers the effect of stub spacing and conductor size for a given termination. A termination of $10^4 \Omega$ at T and $10^{-3} \Omega$ at R is used in all calculations.

Figure 15 gives the maximum attenuation as a function of the spacing D for different radii R_2 of the stub.

It is seen that the maximum attenuation increases moderately with the stub spacing but much more with the stub conductor size.

Bandwidths at three different attenuation levels, 3dB, 6dB and 9dB, as functions of the spacing D, and with R_2/R_1 as a parameter, are illustrated in Figure 16. It is seen that the bandwidth increases with the stub spacing and the conductor size. However, the increase with the conductor size is more pronounced for small stub spacings. For example, at the 6dB level for a 0.5 ft. spacing the bandwidth increases from about 5% to 9% (80% relative change) if the stub diameter is increased from 0.375 in. to 3 in. For a 3 ft. spacing and the same change of

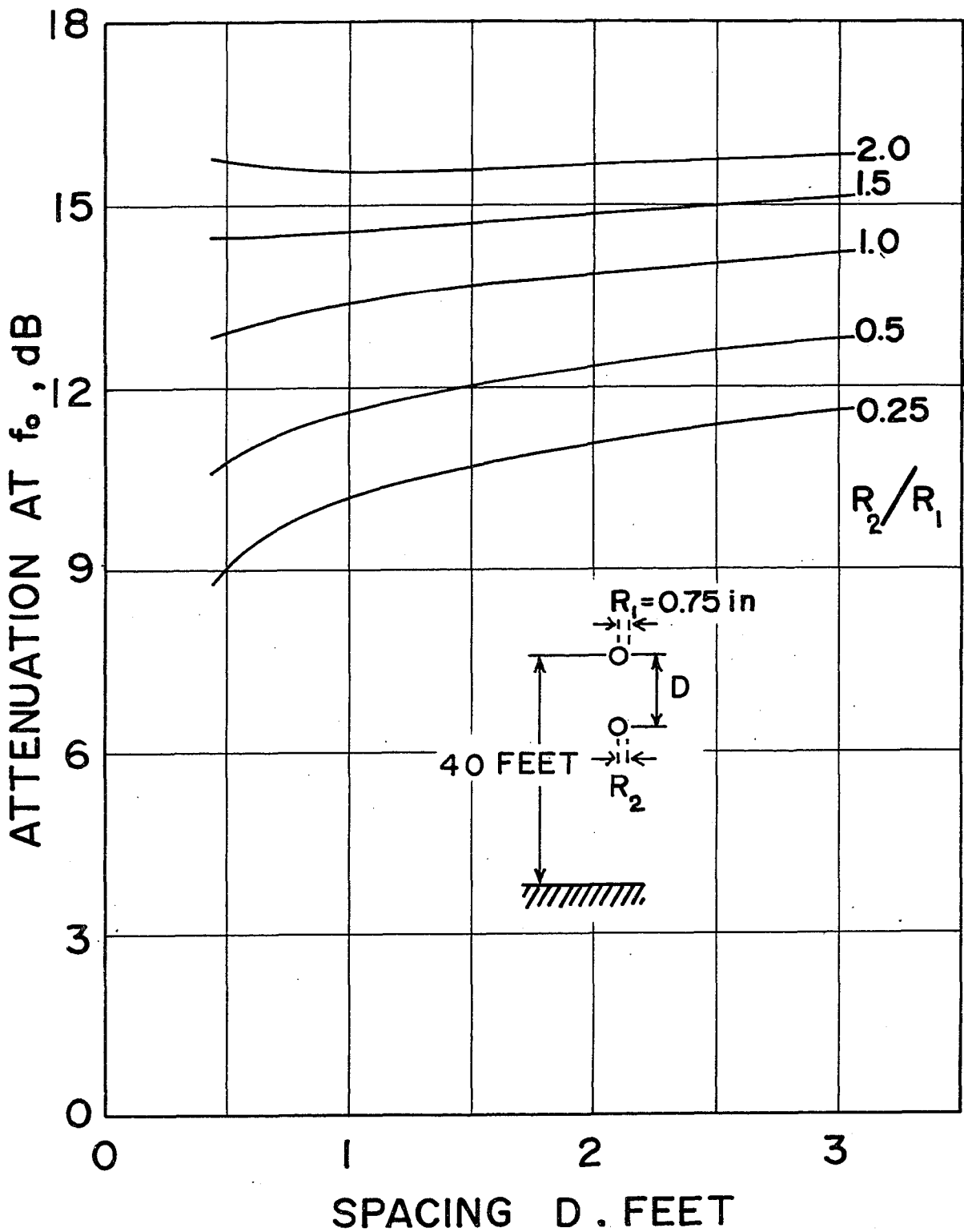


Fig. 15. Effect of Stub-Conductor Spacing on Attenuation at Resonance Frequency f_0 , (Resistive Termination at T, $R_T = 10^4$ Ohms).

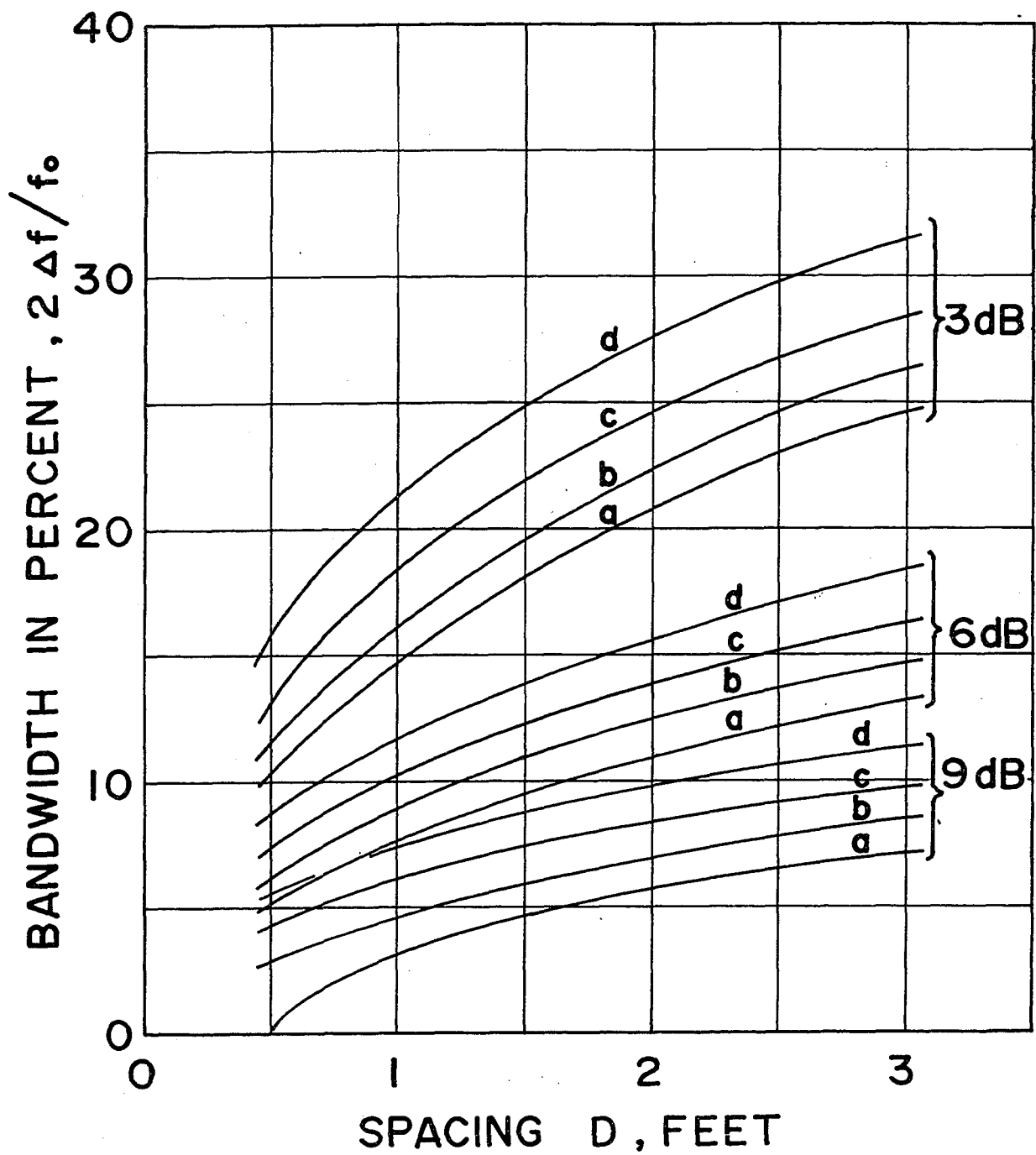


Fig. 16. Effect of Stub-Conductor Spacing on Bandwidth, for a , b , c and d equal to R_2/R_1 , 0.25, 0.50, 1.0 and 2.0 respectively.

conductor size the corresponding bandwidths are about 13% and 18% (38% relative change).

From the study of the effect of filter termination and filter geometry it can be concluded, that the quarter-wave filter performance is determined mainly by the filter geometry, and once the latter is fixed, there exists an optimum termination which is not too critical.

Performance on Multi-Phase Lines

Frequency response curves have been computed for single-, two- and three-phase lines with the geometry of the basic line. The horizontal multiphase lines consist of two or three single-phase basic lines 40 ft apart. The filter is considered to be in the centre of a reflection-free lossless line. The method of calculation is summarized in Appendix A. All conductors and stubs are of the same diameter, 1.5 in., and each single phase filter is terminated at the T-end with a 10kilohm resistor and a very small, 10^{-3} ohm, resistor at the R-end. The effect of this small resistance is insignificant. The stub-to-main conductor spacing is 18 in.

Since any set of conductor input voltage components V_A^i in equation (66) can be resolved into sets of independent natural mode components, filter response curves are computed for natural modes of Line 1.

Figure 17 illustrates the frequency response curves for the ground mode (1), and the "metallic" mode (2) of a two-phase line. The modal incident voltages are, equation (66)

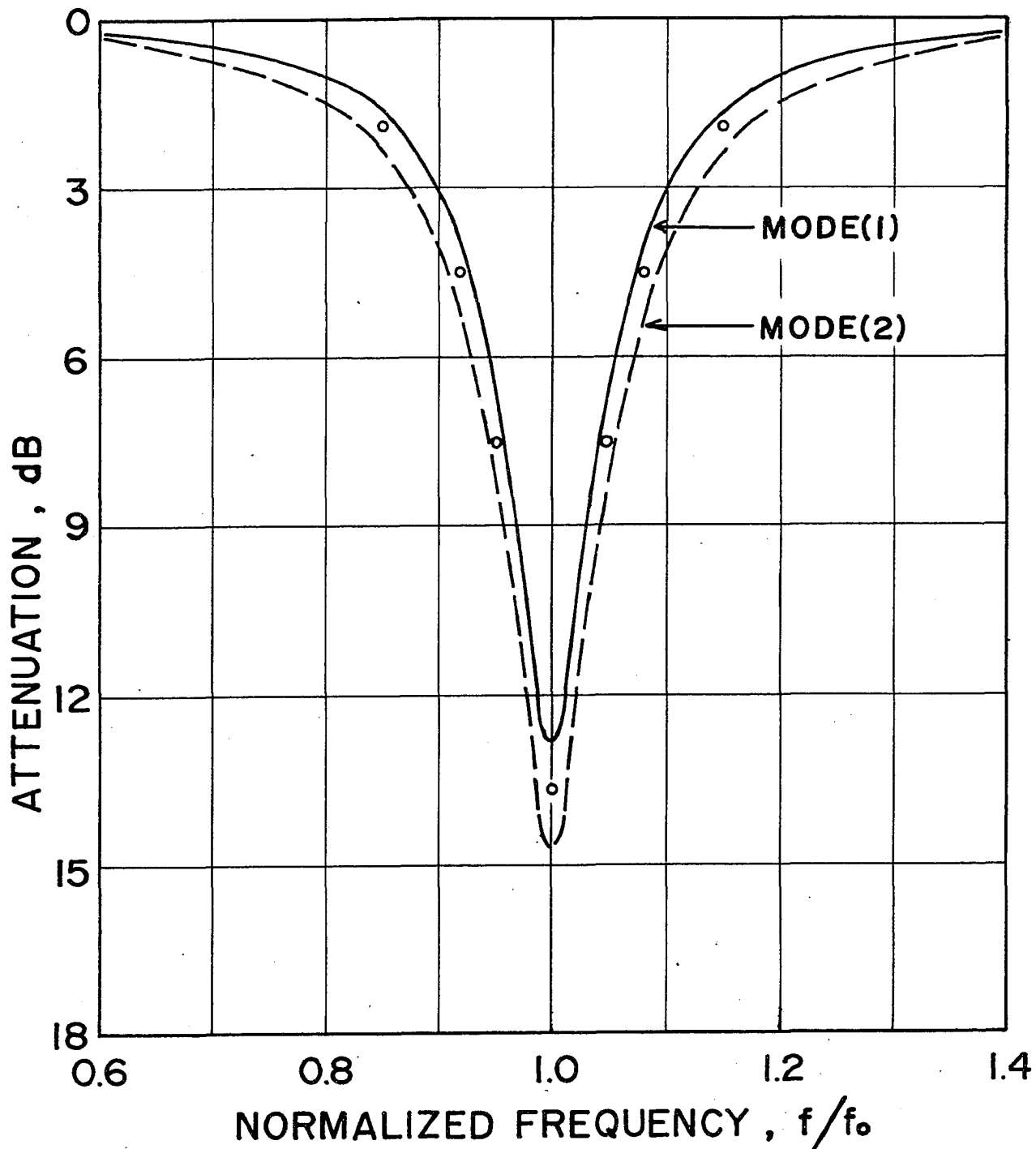


Fig. 17. Modal Frequency Response Curves on Two-Phase Lines, Points Refer to Single-Phase Line Response.

$$V_A^{(1)} = \begin{bmatrix} 1.0 \\ 1.0 \end{bmatrix}; \quad V_A^{(2)} = \begin{bmatrix} 1.0 \\ -1.0 \end{bmatrix}$$

The filter performance for mode (2), the lower curve, is better, with respect to attenuation and bandwidth, than that for mode (1). It is interesting to compare these frequency responses with the response of the basic single-phase line. For clarity, only a few points for the single-phase line are shown in Figure 17. The frequency response for the single-phase line lies between the two modal responses of the two-phase line, and it is nearer the mode (1) response curve. Hence, it may be concluded that the Q-W filter for any set of conductor voltages on a two-phase line is about as efficient as the same filter on a single-phase line. Furthermore, for an approximate preliminary prediction of filter performance on a two-phase line it is sufficient to carry out a single-phase line analysis. This is a convenient simplification that generally will lead to results on the pessimistic side.

There are only two modal curves in Figure 17. Each of the curves applies to either conductor.

Figure 18 illustrates the response curves for the three modes of the horizontal lines for

$$V_A^{(1)} = \begin{bmatrix} 1.000 \\ 1.215 \\ 1.000 \end{bmatrix}; \quad V_A^{(2)} = \begin{bmatrix} 1.0 \\ 0 \\ -1.0 \end{bmatrix}; \quad V_A^{(3)} = \begin{bmatrix} 1.000 \\ -1.645 \\ 1.000 \end{bmatrix}$$

Similarly to the two-phase line only one modal response

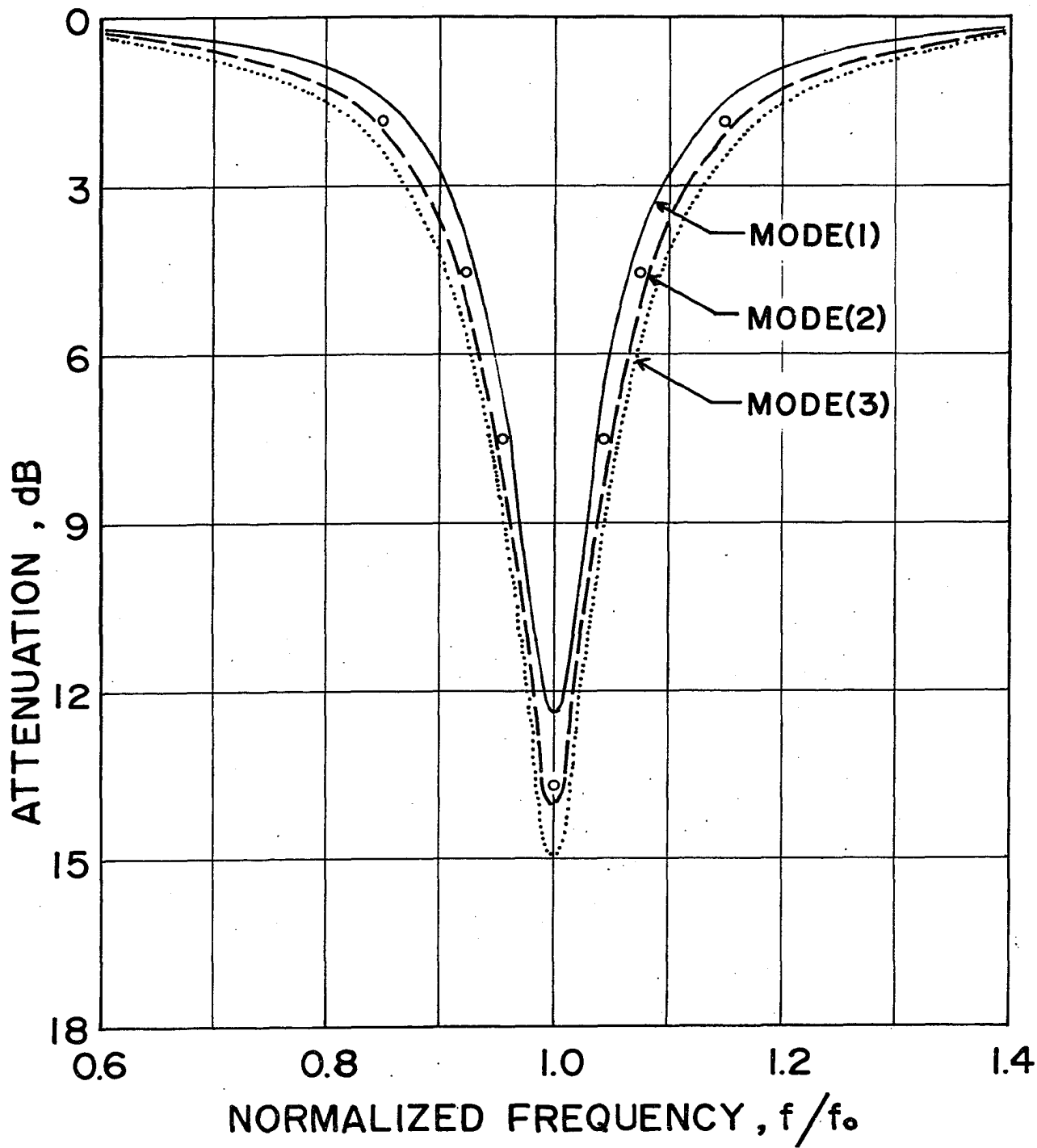


Fig. 18. Modal Frequency Response Curves on Three-Phase Line, Points Refer to Single-Phase Line Response.

curve applies to any of the three line conductors and, hence, only three curves are shown. It was found that with a very good approximation a modal voltage at the filter input produced an attenuated modal output. Hence, the quarter wave filters on a horizontal line are nearly modal-invariant. This finding is not directly evident from the analysis but has been confirmed by detailed calculations.

The three modal curves in Figure 18 indicate again that the mode (1) or ground mode response on the three-phase horizontal line is somewhat inferior to the single-phase line response. On the contrary, the mode (2) and mode (3) response curves are characterized by larger attenuation for any band-width than that for a single line filter. Hence, similarly to a two-phase line, an approximate filter response on a three-phase horizontal line can be found from a simplified analysis applied to a single-phase line.

It was also found that although the phase angles of the conductor components at the filter output change with frequency, the phase shift caused by the filter is nearly the same for each mode. The difference is less than ± 5 degrees for attenuations above 3 db and, hence, it may be neglected. This simplifies the calculation of the resultant conductor voltages from modal components at the filter output. The similarity of relative phase ratios of the input and output components indicates that the filter does not produce any serious interaction between the natural modes of Line 1.

In conclusion, it was found that the performance of Q-W filters

on multiphase horizontal lines can be assessed approximately from the results derived for a single-phase line.

CHAPTER 6

RESUME AND CONCLUSIONS

Two analytical methods are described for the study of quarter wave (Q-W) filters on multiphase power lines. The Direct Method lends itself better for calculations than the Detailed Method. Both methods give identical results.

The analysis is applied to the single-phase, reduced scale test line filters, recently investigated in Japan. The calculated results are compared with the reported measurement data¹. A good agreement is found between the calculated and experimental results.

The application of the analytical method to filters on representative single-, two- and three-phase full-scale lines leads to the following conclusions:

1. The Q-W filter provides a practical means to substantially attenuate high frequencies on power lines.
2. The filter performance is mainly governed by practical considerations of the size of the stubs and their separation from phase conductors. The attenuation and bandwidth increase with increasing stub diameter and separation distance.
3. For any filter geometry, there exists an optimum value of terminating resistance that is connected between the end of the stub and the phase conductor. The value of the terminating resistance is not critical for practical bandwidths.

4. A preliminary approximate determination of the performance and design criteria for filters on multi-phase lines can be deduced from a simpler analysis of a filter on a single-phase line.
5. A broad-band attenuation can be expected with staggered-tuned filters in cascade. This is confirmed by experimental findings on filters installed and operated on a 250 KV 3-phase line.
6. The effective length of the stub and, hence, the principal resonance frequency can be adjusted by a variable capacitive termination.
7. The filter operates at the odd harmonics of the principal resonance frequency.

The broad-band operation of the filters may be useful in the separating of a quiet section of power line from high radio interference level sections.

Possibly the most attractive advantage of the Q-W filters is that the stubs do not carry the line current and, hence, they can be constructed of light hollow conductors. Furthermore, although the stubs are at line potential, no special construction of expensive insulated mounting is required. These two advantages of the quarter-wave filters are of economical significance when compared with conventional wave-traps used in PLC applications.

Finally, the analysis presented in this thesis can be adapted to future analytical investigations of special discontinuities on transmission lines. For example, line-type couplers, transmission line faults and similar problems could be solved.

REFERENCES

1. Sawada, Y., Nakamura, H., "Development of a new wave trap by parallel conductors", Abbreviated English translation, ELECTROTECHNICAL JOURNAL OF JAPAN, Vol 8, No. 1/2, 1963.
2. Perz, M. C., "A method of analysis of power line carrier problems on three-phase lines", IEEE TRANS. POWER APPARATUS AND SYSTEMS, Vol.83, pp.686-691, July 1964.
3. Barthold, L. O., "Radio-frequency propagation on polyphase lines", Ibid., pp. 665-671.
4. Perz, M. C., "Natural modes of power line carrier on horizontal three-phase lines", Ibid., pp. 679-686.
5. Bewley, L. V., "Travelling Waves on Transmission Systems", John Wiley and Sons., New York, 1951.

APPENDIX A
DIRECT METHOD

The body of the thesis consists mainly of general solutions of boundary problems leading to equation (66). This equation has to be evaluated for any discrete value of frequency f .

The analytical study of filter performance requires the use of a digital computer for the operation of matrices with complex entries. To facilitate the computer programming, a step-by-step procedure for the evaluation of the necessary constants in equation (66) is briefly outlined in this Appendix.

In the evaluation of filter performance, the power line constants of Line 1 and 3 are either known a priori or are calculated from classical equations. With the known values of Z_1 , Z_2 , Z_3 and termination lumped admittances at the T and R end of the filter, *the step-by-step procedure is:*

STEP 1. The inverse matrices of Z_1 , Z_2 and Z_3 are calculated

$$Y_1 = Z_1^{-1}$$

$$Y_2 = Z_2^{-1}$$

$$Y_3 = Z_3^{-1}$$

STEP 2. The effective admittance matrix y at R is calculated, equation (13),

$$y = \begin{bmatrix} y_{\ell} + Y_3 & -y_{\ell} \\ y_{\ell} & y_{\ell} \end{bmatrix}$$

STEP 3. Equation (55) is evaluated for the desired frequency f .

$$P = \begin{bmatrix} P_{\ell\ell} & P_{\ell s} \\ P_{s\ell} & P_{ss} \end{bmatrix} = (a + by)^{-1} = (\cos\beta L + j \sin\beta L z_2 y)^{-1}$$

$$\text{where } \beta L = \frac{\pi}{2} \frac{f}{f_0}$$

STEP 4. The input admittance matrix Y_B is determined, equation (40).

$$\begin{aligned} Y_B &= (c + ay)(a + by)^{-1} = (c + ay)P \\ &= (j \sin\beta L Y_2 + \cos\beta L y)P \end{aligned}$$

The total input admittance at T, Y , equation (44) is

$$Y = Y_T + Y_B$$

where

$$Y_T = \begin{bmatrix} Y_\ell & -Y_\ell \\ -Y_\ell & Y_\ell \end{bmatrix}$$

The inverse of Y is

$$Z = Y^{-1} = \begin{bmatrix} z_{\ell\ell} & z_{\ell s} \\ z_{s\ell} & z_{ss} \end{bmatrix}$$

These steps provide the information necessary to calculate the voltage after the filter, v_D , using equation (66).

Calculations in this thesis were made for Lines 1 and 3 identical and reflection-free at the far ends. Hence, Z_3 is the surge impedance of Line 3 and equal to Z_1 . Furthermore, the input impedance of the extended Line 3, Z_{3e} , is also equal to Z_1 .

$$Z_1 = Z_3 = Z_{3e}$$

$$\text{therefore } Z_1 Z_{3e}^{-1} = Z_1 Z_1^{-1} = 1$$

equation (66) reduces to

$$v_D = 2(P_{\ell\ell} + P_{e_s} Z_{s\ell} Z_{\ell\ell}^{-1})(Z_1 Z_{\ell\ell}^{-1} + 1)^{-1} v'_A$$

STEP 5. Finally, the attenuation in dB at the frequency f of each line voltage component is obtained.

$$b_f = 20 \log_{10} \left(\frac{v_D}{v'_A} \right) \text{ (dB)}$$

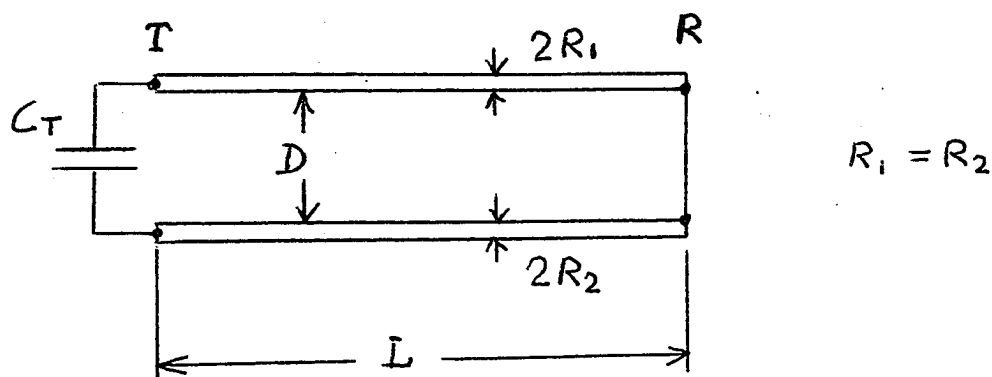
$\frac{v_D}{v'_A}$ is a component by component division and not a

matrix division.

APPENDIX B
CAPACITIVE TERMINATION

A method is derived here how to calculate the capacitance for a desired change of resonance frequency. The filter is assumed shorted at one end and terminated with a capacitor, C_T , at the other end.

At the new resonance frequency, f_r , the filter can be considered as a shorted two-conductor stub line of length L terminated with a capacitor C_T .



The input impedance of the shorted stub is

$$Z_b = jZ_s \tan \beta L$$

where $Z_s = 120 \ln \frac{D}{\sqrt{R_1 R_2}}$ is the surge impedance of the two-conductor line. Let Z_c be the impedance of the capacitor C_T at the frequency f_r .

The condition for resonance is

$$j\omega(Z_c + Z_b) = 0$$

$$\frac{1}{j2\pi f_r C_T} + j Z_s \tan \frac{\pi}{2} \frac{f_r}{f_o} = 0$$

f_o is the resonance frequency of the filter without C_T

$$C_T = \frac{1}{2\pi f_r Z_s \tan \frac{\pi}{2} \frac{f_r}{f_o}}$$

This equation has a physically meaningful solution for $f_r < f_o$ because for $f_r > f_o$, $\tan \frac{\pi}{2} \frac{f_r}{f_o} < 0$, and the value of C_T must be ≥ 0 .

VITA AUCTORIS

- 1943 Born in Yugooslavia.
- 1955 Completes Elementary Education in Argentina.
- 1960 Completes High School in Argentina.
- 1969 B.A.Sc. in Electrical Eng. at the University of Windsor.
- 1970 Candidate for M.A.Sc. in Electrical Eng. at the University of Windsor.